

## Thermal and crustal evolution of Mars

Steven A. Hauck II<sup>1</sup> and Roger J. Phillips

McDonnell Center for the Space Sciences and Department of Earth and Planetary Sciences, Washington University, Saint Louis, Missouri, USA

Received 11 October 2001; revised 4 February 2002; accepted 11 February 2002; published 16 July 2002.

[1] We present a coupled thermal-magmatic model for the evolution of Mars' mantle and crust that may be consistent with estimates of the average crustal thickness and crustal growth rate. By coupling a simple parameterized model of mantle convection to a batch-melting model for peridotite, we can investigate potential conditions and evolutionary paths of the crust and mantle in a coupled thermal-magmatic system. On the basis of recent geophysical and geochemical studies, we constrain our models to have average crustal thicknesses between 50 and 100 km that were mostly formed by 4 Ga. Our nominal model is an attempt to satisfy these constraints with a relatively simple set of conditions. Key elements of this model are the inclusion of the energetics of melting, a wet (weak) mantle rheology, self-consistent fractionation of heat-producing elements to the crust, and a near-chondritic abundance of those elements. The latent heat of melting mantle material is a small (percent level) contributor to the total planetary energy budget over 4.5 Gyr but is crucial for constraining the thermal and magmatic history of Mars. Our nominal model predicts an average crustal thickness of  $\sim 62$  km that was 73% emplaced by 4 Ga. However, if Mars had a primary crust enriched in heat-producing elements, consistent with SNC meteorite geochemistry, then our models predict a considerably diminished amount of post 4 Ga crustal emplacement relative to the nominal model. The importance of a wet mantle in satisfying the basic constraints of Mars' thermal and crustal evolution suggests (independently from traditional geomorphology or meteorite geochemistry arguments) that early Mars had a wet environment. Extraction of water from the mantle of a one-plate planet such as Mars is found to be extremely inefficient, such that 90–95% of all water present in the mantle after the initial degassing event should still reside there currently. Yet extraction of even 5% of a modestly wet mantle ( $\sim 36$  ppm water) would result in a significant amount (6.4 m equivalent global layer) of water available to influence the early surface and climate evolution of the planet. *INDEX TERMS:* 6055 Planetology: Comets and Small Bodies: Surfaces and interiors; 6225 Planetology: Solar System Objects: Mars; 5455 Planetology: Solid Surface Planets: Origin and evolution; 8130 Tectonophysics: Evolution of the Earth: Heat generation and transport; 8147 Tectonophysics: Evolution of the Earth: Planetary interiors (5430, 5724); *KEYWORDS:* Mars, mantle convection, thermal evolution, crust, partial melting

### 1. Introduction

[2] The coupled evolution of the mantle and crust is one of the most significant problems in the geodynamics of terrestrial planets [e.g., *Lenardic and Moresi, 1999*]. A primary area of interest is the role that crustal genesis has on the thermal evolution of a planet [e.g., *DeSmet et al., 1999*], as well as the form that it takes as a result of the dominant mantle dynamical regime. Observations of the known terrestrial planets allude to at least two end-member regimes of mantle-crust evolution. Earth's own plate tectonics represents ongoing crustal production and destruction

over at least hundreds of millions, and likely billions, of years. Recycling of the crust and lithosphere efficiently cools and reincorporates many evolved compositional components into the mantle. Mercury, Venus, and Mars, at present, seem to represent something quite different: one-plate planets that lack evidence of plate tectonics like mid-ocean ridges or subduction zones. The surfaces of each, however, vary greatly, from ancient Mercury to the more youthful Venus. Mars' evolution provides a host of interesting mysteries with its ancient southern highlands, the vast and rapidly emplaced Tharsis complex, and its seemingly water-carved landscape despite the present-day instability of water. Its many mysteries and the opportunities provided by results from the Mars Global Surveyor (MGS) spacecraft lead us to attempt to understand the conditions of its thermal and magmatic evolution.

[3] Mars' thermal evolution presents an interesting enigma. A comparison of seemingly reasonable Martian

<sup>1</sup>Now at Department of Terrestrial Magnetism, Carnegie Institution of Washington, Washington, D. C., USA.

geotherms derived from thermal history calculations with available mantle phase relations reveals the potential for significant, widespread mantle melting throughout time [e.g., Reese *et al.*, 1998; Choblet *et al.*, 1999; Hauck and Phillips, 2000; Weizman *et al.*, 2001]. While small amounts of partial melting in the mantle are conceivable (e.g., Earth), these results suggest the potential for maximum melt fractions of several tens of percent and maximum depths of melting of several hundred kilometers. This result appears to be contrary to the surface view of Mars with its ancient, Noachian (>3.5 Ga) highlands covering at least 40% of the planet and the 1–2 order of magnitude decrease in post-Noachian volcanic resurfacing [Tanaka *et al.*, 1992]. There is, however, evidence of young volcanic flows (10–100 Ma) [Hartmann *et al.*, 1999], suggesting that the planet may still be volcanically active at infrequent intervals.

[4] The issue of whether a Martian melting paradox exists is significant because it affects our ability to link ideas about the inferred geological and geophysical history. We recognize that any potential solution to this paradox may suffer from its own nonuniqueness. However, a wealth of observations, from knowledge of Martian meteorites [e.g., McSween, 1994] to recent MGS derived gravity and topography inversions for internal structure [Zuber *et al.*, 2000] to knowledge of surface evolution [Tanaka *et al.*, 1992], may allow us to place some bounds on reasonable thermal history models. While other workers [Stevenson *et al.*, 1983; Schubert and Spohn, 1990; Schubert *et al.*, 1992] have approached the problem of Mars' thermal history in the past, we implement recent understanding of how the mantles of one-plate planets may convect [Solomatov, 1995; Reese *et al.*, 1998, 1999; Solomatov and Moresi, 1996, 2000; Grasset and Parmentier, 1998]. In addition, we recognize that the thermal history of the planet is intimately coupled to its magmatic history via both the thermodynamics of melting and the surface record. Evidence of water's role in shaping the planet is pervasive [e.g., Carr, 1996], and owing to the significant effect it has on the rheology of rocks [e.g., Chopra and Patterson, 1984; Karato and Wu, 1993; Hirth and Kohlstedt, 1996; Mackwell *et al.*, 1998; Mei and Kohlstedt, 2000a, 2000b], it too may have a prominent role in Mars' thermal evolution.

[5] We address several important aspects in understanding the thermal evolution of a small, one-plate planet such as Mars. First, among models of Mars bulk composition, estimates for the primary heat-producing elements of K, U, and Th vary considerably (especially K) and hence so does the thermal energy budget of the mantle. Second, melt production is potentially a significant energy sink owing to the latent heat of melting, yet it has been neglected in previous Martian thermal history models [e.g., Stevenson *et al.*, 1983; Schubert and Spohn, 1990; Schubert *et al.*, 1992]. Third, we study how differentiation of heat-producing elements into the crust consistent with predicted degrees of mantle melting affects the thermal and magmatic evolution. Fourth, the rheology of the mantle (which may be governed by water content) is a primary control on thermal evolution of the mantle. Thus we address post-formational volatile degassing and its implications for planetary evolution.

## 2. Modeling

[6] We adopt the approach of modeling planetary thermal evolution via a parameterized convection scheme [e.g., Phillips and Malin, 1983; Stevenson *et al.*, 1983; Schubert and Spohn, 1990]. We assume that Mars was initially hot such that differentiation of the core and mantle occurred very early, consistent with estimates for Martian core formation [Chen and Wasserburg, 1986; Lee and Halliday, 1997]. We utilize the core cooling and inner core formation model of Stevenson *et al.* [1983]. A partial melt model [McKenzie and Bickle, 1988] is coupled to a parameterized convection model [Phillips and Hansen, 1998; Hauck and Phillips, 2000; Phillips *et al.*, 2001a] so that we may investigate both the thermal and magmatic evolution of the planet.

[7] Our approach is to utilize a one-dimensional (radial dimension) model of convection in a spherical shell overlaying a spherical core. We assume whole mantle convection, which is parameterized via a relationship between the Rayleigh number ( $Ra$ ) and the Nusselt number ( $Nu$ ) [e.g., Turcotte and Schubert, 1982]. This relationship describes how the vigor of convection relates to the efficiency of convective heat transfer. The equations for the conservation of energy are solved as a function of time for a cooling (and potentially solidifying) core, a convecting mantle, and a thickening (or thinning) upper boundary layer representing the lithosphere. Our model is essentially the same as that described by Stevenson *et al.* [1983], including their formulation for core cooling and inner core formation with three main enhancements. First, we explicitly include the latent heat energy involved in melting in the equation for the mantle energy balance. Second, instead of the thin-lid, constant viscosity scaling of the  $Ra$ - $Nu$  relationship that Stevenson *et al.* [1983] used, which may be more appropriate for a planet with plate tectonics, we utilize recently described scaling relationships for fluids with highly temperature-dependent viscosity. These relationships, for a regime known as stagnant lid convection, are likely more appropriate for one-plate planets with an immobile lithosphere over a convecting mantle [Solomatov and Moresi, 1996, 2000; Schubert *et al.*, 1997; Reese *et al.*, 1998, 1999; Grasset and Parmentier, 1998]. Assuming extraction of melt, the latent heat of melting is an energy sink for the mantle and an energy source in the crust. Third, instead of assuming a linear temperature profile through the lithosphere (upper boundary layer), we use a one-dimensional (1-D) adaptive remeshing finite element solution for the advection-diffusion equation. This scheme allows us to capture the physics of the thickening (or thinning) of the lid as well as introduce depth and temperature dependence for material properties such as heat production and thermal conductivity.

### 2.1. Parameterized Mantle Convection

[8] The methodology for the parameterized convection scheme is standard [e.g., Phillips and Malin, 1983; Stevenson *et al.*, 1983; Schubert and Spohn, 1990; Schubert *et al.*, 1992; Phillips and Hansen, 1998; Reese *et al.*, 1999] and is described in detail by Stevenson *et al.* [1983]. Equation (1) is the differential equation for conservation of energy in the mantle. We explicitly include the term for the effect of the latent heat of melting, which is a modification of previous models of parameterized thermal evolution. Melt production

is calculated using the methodology of *McKenzie and Bickle* [1988] and is further described in sections 2.5 and 2.6:

$$\frac{4}{3}\pi(R_p^3 - R_c^3)\left[H - \rho_m c_m \frac{d\langle T_m \rangle}{dt}\right] - \rho_m f_{pm} L_{pm} = 4\pi(q_s R_p^2 - q_c R_c^2). \quad (1)$$

The radii of the planet and of the core are  $R_p$  and  $R_c$ , respectively.  $H$  is the specific (per unit volume) heat production, and  $\rho_m$  and  $c_m$  are the density and heat capacity of the mantle. The average mantle temperature is  $\langle T_m \rangle$ ,  $f_{pm}$  is the volumetric melt production, and  $L_{pm}$  is the latent heat of melting. The surface and core heat fluxes are given by  $q_s$  and  $q_c$ .

[9] The solution of equation (1) is parameterized by a relationship between the Rayleigh number ( $Ra$ ) and the Nusselt number ( $Nu$ ):

$$Nu = a\theta^b Ra^c. \quad (2)$$

The constants  $a$ ,  $b$ , and  $c$  vary as a function of convective regime and can vary with the stress dependence of viscosity [e.g., *Solomatov and Moresi*, 2000]. The parameter  $\theta$  describes the natural logarithm of the viscosity contrast, which is important in the description of convective heat transfer in fluids with large viscosity variations such as those that can lead to stagnant lid convection [*Solomatov*, 1995]. The ratio of buoyancy forces to viscous forces known as the Rayleigh number can be defined as follows:

$$Ra = \frac{ga(\Delta T)d^3}{\eta\kappa}. \quad (3)$$

The  $Ra$  number is dependent on the gravity,  $g$ , the coefficient of thermal expansion,  $\alpha$ , the viscosity,  $\eta$ , the thermal diffusivity,  $\kappa$ , the temperature contrast,  $\Delta T$ , and the layer thickness  $d = (R_p - R_c)$ . The Rayleigh number can be subdefined by the temperature used to calculate the viscosity; in the stagnant lid regime an internal Rayleigh number,  $Ra_i$ , is useful where the viscosity is that at the base of the stagnant lid [e.g., *Reese et al.*, 1998, 1999; *Solomatov and Moresi*, 2000].

[10] The Nusselt number, which is the ratio of the total heat flux across the system to the heat that is conducted across it, describes the heat transported across the system. The  $Nu$  number is related to the heat flux supplied to the base of the lid (and additively related to the surface heat flux in a system with crustal and lithospheric heat production) by

$$q_m = Nu \frac{k\Delta T}{d}. \quad (4)$$

Thermal conductivity is given by  $k$ ,  $\Delta T$  is the temperature contrast across the mantle, and the depth of the layer is  $d$ . Hence, because equation (2) provides a relationship between mantle temperature and heat flux, it is possible to simultaneously solve equations (1) and (2) for the state of the system.

[11] Differential equations for the cooling and potential inner core solidification [*Stevenson et al.*, 1983] coupled with equation (1) can be solved as a function of time using a

Runga-Kutta scheme and the relationship between heat flux and internal temperature provided by the parameterization in equations (2)–(4). The solution of these equations provides the evolution of planetary temperatures and heat fluxes over time.

## 2.2. Lithospheric Thickening

[12] Standard parameterized convection models have simply assumed that the lithosphere is in a state of steady conductive heat transfer with negligible contributions due to advection [e.g., *Stevenson et al.*, 1983]. Additionally, most of these models ignore heat production within the crust and lithosphere (cf. *Phillips and Malin* [1983], which did in a simple, analytic manner) and the possibility of variable material properties such as thermal conductivity [i.e., *Hauck et al.*, 1999; *Hofmeister*, 1999]. We allow for these contributions by implementing a finite element scheme [e.g., *Reddy and Gartling*, 1994] with adaptive remeshing to follow the thickening of the lithosphere. We solve the transient, one-dimensional, non-linear, advection-diffusion equation in the lithosphere given by

$$\rho_l c_l \dot{T} = H_l(z) - \nabla \cdot [k(T, z, X)\nabla T]. \quad (5)$$

The density and heat capacity of the lithosphere are  $\rho_l$  and  $c_l$ . The variation of lithospheric heat production,  $H_l$ , is a function of depth,  $z$ . The thermal conductivity can also vary as a function of temperature, depth, and mineralogy if necessary.

[13] Solution with time is accomplished using a standard Crank-Nicholson time-integration method [*Reddy and Gartling*, 1994]. We use a consistent “mass” matrix and can solve the system using a simple tri-diagonal inversion. For the case of variable conductivity, we use the Picard (subsequent substitution) iterative method [*Reddy and Gartling*, 1994] to return solutions for both temperature and thermal conductivity. This method for solving advection-diffusion problems with nonlinear conductivity was used and benchmarked in two dimensions by *Hauck et al.* [1999]. Boundary conditions are simple: a constant temperature at the top of the domain (representing the planetary surface) and a heat flux at the base of the lithosphere equal to that predicted by the parameterized convection model via equation (4). In this one-dimensional model we implicitly assume that there is no heat transport due to the lateral components of conduction and advection. Several different configurations for the variation of heat generation with depth can be implemented (e.g., constant, linear, or exponential decay with depth). We adopt an exponential decay of the concentration of heat producers with depth where the total crustal concentration is governed by the amount extracted from the mantle (see below) and by the imposed requirement that the concentration at the crust-mantle boundary is continuous. This configuration results in an Earth-like crustal model [*Turcotte and Schubert*, 1982] that is numerically well behaved owing to our constraint of continuity of heat production at the crust-mantle boundary.

[14] The adaptive remeshing scheme is governed by two simple principles. First, we require that temperature is continuous at the base of the lithosphere; continuity of heat flux is enforced by the boundary conditions. Second, the finite element domain defines the thermal lithosphere and

**Table 1.** Summary of Stagnant Lid Scaling Parameters for the  $Ra-Nu$  Relationship in Equation (2)

	$a$	$b$	$c$
Steady ( $n = 1$ )	1.89	-1.02	0.2
Time-dependent	$0.31 + 0.22n$	$-2(n + 1)/(n + 2)$	$n/(n + 2)$

vice versa. This is accomplished through a series of iterations of growing (or shrinking) the domain until the temperature at the base of the finite element domain matches the temperature at the top of the mantle from the parameterized convection prediction at the end of any given time step. The elements are of constant length for any iteration, and nodal temperatures are reinterpolated each iteration onto the new mesh. A constant number of elements (500 for all models here) are used within a simulation.

### 2.3. One-Plate Planet Convection

[15] At present, Mars is a one-plate planet, and likely has been for much, if not all, of its history. While there have been suggestions that Mars may have once harbored plate tectonics [Sleep, 1994; Connerney et al., 1999], there is no concrete evidence of whole-scale lithospheric recycling. Convection within a one-plate planet is likely analogous to the stagnant lid regime of convection within a variable viscosity fluid [Solomatov, 1995; Solomatov and Moresi, 1996, 2000; Reese et al., 1998, 1999; Grasset and Parmentier, 1998] that does not contain variable lateral mechanical properties such as elastic or plastic strength [cf. Moresi and Solomatov, 1998]. Stagnant lid convection is a natural consequence of convection within a fluid with large viscosity contrasts especially due to highly temperature-dependent viscosity. In this regime a rigid lid develops near the colder upper boundary layer, where the viscosity is highest; convective motions occur in a sub-layer beneath the rigid lid. By its very nature, stagnant lid convection is considerably less efficient at transporting heat out of the system relative to one where the advection of heat via recycling of the whole thermal boundary layer is accomplished. All heat lost from this system must necessarily be transported via conduction across the rigid lid. Significant advances in the understanding of convection in this regime have been accomplished recently via experiments [e.g., Davaille and Jaupart, 1993; Solomatov and Moresi, 2000]. For the purpose of modeling Mars' thermal evolution, we explicitly assume that most of its history was governed by heat transport via stagnant lid convection. We adopt the scaling relationships revealed by experiments (e.g., the review by Solomatov and Moresi [2000]) for parameterizing convection through equation (2).

[16] Stagnant lid convection can occur in two regimes: steady and time-dependent. Their general heat transport efficiencies are governed by the  $Ra-Nu$  relationship. Table 1 lists the appropriate parameters for  $a$ ,  $b$ , and  $c$  in equation (2) for stagnant lid convection [Grasset and Parmentier, 1998; Reese et al., 1998, 1999; Solomatov and Moresi, 2000]. In addition to dependence on the Rayleigh number and viscosity variations, the efficiency of heat transfer is dependent on the viscous flow regime of the mantle. The parameters that govern equation (2) are dependent on the exponent of the stress dependence of viscosity,  $n$ . Most of

the calculations here are for time-dependent convection; however, we also investigate the effects of steady convection using the numerical results of Solomatov and Moresi [1996] for a Newtonian fluid for comparison.

### 2.4. Viscosity

[17] In addition to the scaling relationships, a constitutive relationship for viscosity is needed to describe fully mantle flow and heat transport. As a first-order approximation, we assume that solid-state creep of olivine dominates the flow of rocks within the Martian mantle. While the interior of Mars may have a larger normative fraction of pyroxene than the Earth [e.g., Sanloup et al., 1999], any significant fraction of olivine may control mantle deformation due to its weakness relative to pyroxenes [Mackwell, 1991]. Mantle viscosity, which is predominantly governed by the solid-state creep of olivine [e.g., Karato and Wu, 1993], can be described by

$$\eta = \frac{\mu^n}{3^{(n+1)/2} A^*} \left(\frac{1}{\sigma}\right)^{n-1} \left(\frac{h}{B^*}\right)^m \exp\left(\frac{E + PV}{RT}\right). \quad (6)$$

The shear modulus is  $\mu$ , the grain size is  $h$ , and the Burger's vector is  $B^*$ .  $A^*$  is an experimentally derived constant, and  $\sigma$  is the driving stress, or, more rigorously, the square root of the second invariant of the deviatoric stress tensor. The exponential dependence of the viscosity on stress and grain size is given by  $n$  and  $m$ , respectively. The numerical prefactor is due to the necessary geometric proportionality factor needed to relate the equivalent stress measured in experiments with the square root of the second invariant of the deviatoric stress tensor [Ranalli, 1995]. The viscosity depends exponentially on the activation enthalpy  $Q = E + PV$ , where  $E$  is the activation energy,  $P$  is the pressure, and  $V$  is the activation volume. The activation enthalpy is often approximated as a constant where  $P$  is a representative pressure [Reese et al., 1999], as is done here. The universal gas constant is  $R$ , and the temperature is  $T$ . We also employ the definition of an internal Rayleigh number based on the temperature at the bottom of the lithosphere for proper use of the stagnant lid relationships [Solomatov, 1995; Solomatov and Moresi, 1996, 2000; Reese et al., 1999].

[18] Viscosity variations within the system govern the transport of heat out of the planet by the development of a cold, rigid surface boundary layer. The functional dependence of heat transport on convective vigor within a system with strongly varying viscosity is arrived at by relating the viscosity variation across the system to the smaller viscosity (and temperature) contrasts that are involved in active convection beneath the more rigid lid. This dependence has been shown through boundary layer theory [Solomatov, 1995] and in experiments [Davaille and Jaupart, 1993]. The parameter  $\theta$  from equation (2) is simply the natural logarithm of the viscosity contrast due to the temperature contrast across the upper boundary layer:

$$\theta = \ln(\Delta\eta). \quad (7)$$

[19] A way to understand the physical significance of this parameter is to recognize its role in how convection is

driven beneath the more rigid lid. Convection beneath a stagnant lid is driven by the temperature difference across a smaller sublayer at the base of the lid that participates in the convective flow. This smaller, more participatory boundary layer can be understood via analogy to be similar to the cold boundary layer in an isoviscous fluid that participates in the large-scale convective flow. The temperature difference necessary to drive convection within a variable viscosity fluid is intimately tied to how the viscosity varies with temperature. Therefore we can relate  $\theta$  to the temperature contrast in this sub-layer using the following equation where  $\Delta T_{sl}$  the temperature contrast across the sublayer and  $a_{sl}$  is a constant ( $\sim 2.2$ ) estimated from experiments [e.g., *Davaille and Jaupart*, 1993; *Solomatov*, 1995; *Grasset and Parmentier*, 1998]:

$$\Delta T_{sl} = a_{sl}\theta^{-1}. \quad (8)$$

## 2.5. Melting Model

[20] We use a simple, well-known model for the generation of partial melt due to adiabatic decompression [*McKenzie and Bickle*, 1988; *McKenzie*, 1984]. While this model does not completely describe the thermodynamic energetics of multicomponent melting even in isentropic systems [e.g., *Asimow et al.*, 1995; *Hirschmann et al.*, 1999], it is appropriate enough to learn something about the overall melt productivity [*Hirschmann et al.*, 1999]. Recent experiments on the phase relations of peridotite have provided better constraints on the liquidus and solidus, as well as extending results to higher pressures [*Zhang and Herzberg*, 1994; *Herzberg et al.*, 2000; *Hirschmann*, 2000].

[21] In particular, we use the basic KLB-1 phase diagram derived by *Zhang and Herzberg* [1994]. These results, especially at high pressures, are noticeably different from the parameterizations used by *McKenzie and Bickle* [1988], partially owing to composition, but also experimental technique [*Zhang and Herzberg*, 1994]. More recent estimates for the peridotite solidus exist owing to the review and reanalysis by *Hirschmann* [2000] and new experiments by *Herzberg et al.* [2000]. However, despite the fact that differences among parameterizations of *Zhang and Herzberg* [1994], *Herzberg et al.* [2000], and *Hirschmann* [2000] at high pressures are up to 50 K, which is within  $2\sigma$  error (up to 50–70 K) [*Herzberg et al.*, 2000; *Hirschmann*, 2000]. Regardless of which post-1988 parameterization we utilize, the results are significantly different than if we were to adopt the *McKenzie and Bickle* [1988] parameterization. This result is principally due to the unconstrained extrapolation to high pressures, which has been alleviated by the more recent experiments. An important upshot is that predictions of runaway mantle melting [e.g., *Phillips et al.*, 2001a] due to a mantle temperature gradient in excess of the solidus temperature gradient (at high pressures) are not seen in our models. This problem is avoided by coupling the updated peridotite phase relations for KLB-1 of *Zhang and Herzberg* [1994] with the methodology for the calculation of partial melt developed by *McKenzie and Bickle* [1988] and *McKenzie* [1984].

[22] The Martian mantle is likely to be much more iron-rich than the Earth's [e.g., *Wänke and Dreibus*, 1994;

*Lodders and Fegley*, 1997]. Estimates for the Mg # (= Mg/(Fe + Mg)) of the Martian mantle are near 75 as opposed to almost 90 for the Earth. This difference in Mg # might suggest that the use of terrestrial peridotite as an analog for the Martian mantle is inappropriate. However, results of melting experiments on materials of presumed Martian composition [*Bertka and Holloway*, 1994a, 1994b] and recent reviews of peridotite melting [*Herzberg et al.*, 2000; *Hirschmann*, 2000] suggest that Mg # has, at best, a very minor influence on the location of the peridotite solidus. Additionally, *Schmerr et al.* [2001] have extended the lower pressure work of *Bertka and Holloway* [1994a] to over 20 GPa and found that the solidus of their more iron-rich material is quite similar to that for KLB-1. This result indicates that despite the likely variations in composition between Mars and Earth mantle materials, use of terrestrial peridotite phase relations is a reasonable analog for the Martian mantle.

## 2.6. Melt Production

[23] In order to properly couple the thermal and melting models, we need a relationship that describes the rate at which melt is produced and extracted. For simplicity, we assume that all melt generated is extracted to form the crust either via extrusion to the surface or subsurface intrusion; therefore the rate of extraction is equal to melt production. As melt in a convecting system is generated dominantly by adiabatic decompression, we limit our models to this process. Adiabatic decompression occurs where material is upwelling. Stagnant lid convection tends to be dominated by regions of passive upwelling and downwelling rather than plumes generated at the core-mantle boundary. Therefore we do not consider the effects of actively upwelling regions with considerably higher temperatures than average mantle. Our melt production calculations simply consider the fluxing of mantle material through a region where the temperature is supersolidus. If we can approximate upwelling mantle as approximately cylindrical and the flux of material through the melt-channel [e.g., *Reese et al.*, 1998] to be directly related to the interior convecting velocity, then we can write a simple relationship for the melt productivity:

$$f_{pm} = \frac{4u_i\phi(d_m)^2}{d^2} A_{\text{planet}}. \quad (9)$$

The melt-channel thickness,  $d_m$ , is the region between the base of the lithosphere and the maximum depth of melting. The average volume fraction of melt is  $\phi$  and is given by the melting relations. The melt fraction can additionally be expressed as a function of depth [*McKenzie*, 1984] and equation (9) given in its integral form. However, for a uniform convecting velocity, the results are not changed. The depth of the convecting layer,  $d$ , is a proxy for convective cell size and provides a reasonable normalization such that the melt productivity may be extended to the whole planet via its surface area,  $A_{\text{planet}}$ . This result is similar to *Reese et al.* [1998], but we have explicitly limited melt generation to regions of upwelling rather than an entire convection cell. We use the following expressions for the scaling of interior convecting velocity in the steady [e.g., *Reese et al.*, 1999]

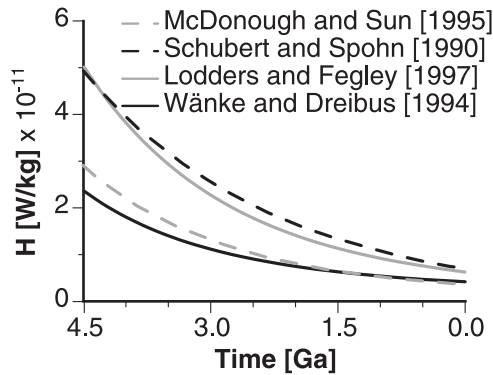


**Figure 1.** Heat production per unit mass as a function of time. *Lodders and Fegley* [1997] and *Wänke and Dreibus* [1994] are for model Mars compositions, *Schubert and Spohn* [1990] represents a composite heat production model applied to Mars, and *McDonough and Sun* [1995] represents a CI chondrite composition. Note the more than a factor of 2 greater heat production of the *Wänke and Dreibus* [1994] composition compared to that of *Lodders and Fegley* [1997].

and time-dependent regimes [*Solomatov and Moresi*, 2000], respectively:

$$u_i = 0.05 \left( \frac{\kappa}{d} \right) \theta^{\frac{-2n}{n+2}} Ra_i^{\frac{2n}{n+2}} \quad (10)$$

$$u_i = \frac{\kappa}{d} (0.04 + 0.34n^{-1}) \left( \frac{Ra_i}{\theta} \right)^{\frac{n(2n+1)}{(n+1)(n+2)}}. \quad (11)$$

## 2.7. Concentration and Distribution of Heat Producers

[24] The concentration and distribution of elements that generate heat via radioactive decay are key aspects of the thermal evolution of planets. The long-lived isotopes of  $^{40}\text{K}$ ,  $^{232}\text{Th}$ , and  $^{235}\text{U}$  and  $^{238}\text{U}$  are principally responsible for the generation of this source of heat. Estimates of the concentration of K, U, and Th within planetary bodies come from studies of the Earth's bulk composition and of meteorites, especially those believed to have been ejected from Mars [e.g., *Wänke and Dreibus*, 1994; *McDonough and Sun*, 1995; *Lodders and Fegley*, 1997, 1998].

[25] There are two distinct classes of heat production models that exist for Mars and that have been employed in the past. The first has nearly chondritic abundances of K, Th, and U; the bulk Mars compositional models of *Wänke and Dreibus* [1994] (WD94) fit into this class. The second is best illustrated by the compositional model of *Lodders and Fegley* [1997] (LF97) but is not considerably different from the simplified heat production model utilized by *Schubert and Spohn* [1990] for a reasonable Martian mantle density (see Figure 1). Table 2 contains the abundance of heat-producing elements for the two classes of models using the results of *Wänke and Dreibus* [1994] and *Lodders and Fegley* [1997], respectively. Estimates for the fraction that each of the radioisotopes makes up for each of the elements and their heat generation rates are taken from *Turcotte and Schubert* [1982]. The major difference among the WD94 and LF97 models concerns the abundance of potassium. The LF97

model predicts over thrice as much K in the bulk silicate portion of the planet than the WD94 model. The effect of this difference in potassium abundance is plainly obvious in Figure 1, where for early in planetary history the difference in heat production rate is approximately a factor of 2.

[26] On the Earth, crustal contributions in stable regions such as continents may account for as much as one half the surface heat flow [e.g., *Turcotte and Schubert*, 1982, p. 147]. This point suggests that upward concentration of heat-producing elements due to differentiation is an important aspect of the global energy balance. Therefore, with our melting model we self-consistently include fractionation of heat-producing elements due to batch melting. We do this in a simple manner, whereby all the heat-producing isotopes are assumed to have the same distribution coefficient between melt and residual solids. The equation for the fractionation due to a batch-melting model is given by

$$C_{\text{melt}} = C_{\text{mantle}} \frac{1}{\phi + D(1 - \phi)}. \quad (12)$$

The concentrations of heat producers in the melt and in the average mantle are  $C_{\text{melt}}$  and  $C_{\text{mantle}}$ , respectively. The bulk distribution coefficient is  $D$  and for incompatible species is generally a value between zero and one.

## 3. Results

[27] In order to gain insight into how a strongly coupled thermomagmatic convecting mantle system behaves, as well as its implications for understanding Mars' history, we perform a parameter-space study for Mars-like conditions. In particular, we investigate the effect of the latent heat of melting, the role of rheology (especially wet versus dry), initial mantle temperature, the distribution coefficient for extraction of heat-producing elements, and concentration of heat-producing elements. Owing to the strong influence of water on rheology and the role water has had in shaping the surface of Mars, we are especially interested in the part that water may have played in the internal evolution of the planet. We begin with a brief discussion of our nominal model, which we believe captures many of the basic features of Mars' evolution. This model is relatively simple in composition and provides a basis for discussing the effects of additional complexities. This discussion is followed by a brief exploration of the effects of the different heat production models. Next, we illustrate the effect that latent heat of melting has on models of coupled thermal and melting histories. We then summarize the effects of varying initial conditions, rheology, convective regime, and the efficiency with which heat producers are extracted from the mantle and concentrated in the crust.

### 3.1. Nominal Thermal and Crustal History Model

[28] Our nominal model is constructed to satisfy several potential constraints on Mars' evolution, some recently

**Table 2.** Summary of Estimate of Heat-Producing Element Concentrations for the Bulk Silicate Portion of Mars

	K, ppm	Th, ppb	U, ppb
Low [ <i>Wänke and Dreibus</i> , 1994]	305	56	16
High [ <i>Lodders and Fegley</i> , 1997]	920	55	16

**Table 3.** Summary of Basic Parameters of the Nominal Model

Parameter	Var.	Value	Units
Radius of planet	$R_p$	$3390 \times 10^3$	m
Radius of core	$R_c$	$1550 \times 10^3$	m
Density of mantle	$\rho_m$	3527	kg/m <sup>3</sup>
Heat capacity of mantle	$c_m$	1149	J/(kg K)
Density of core	$\rho_c$	7200	kg/m <sup>3</sup>
Heat capacity of core	$c_c$	571	J/(kg K)
Core sulfur mass fraction	$\chi_s$	0.15	—
Initial upper mantle temperature	$T_{i0}$	1723	K
Initial CMB temperature	$T_{c0}$	2000	K
Gravitational acceleration	$g$	3.7	m/s <sup>2</sup>
Mantle thermal expansivity	$\alpha$	$2 \times 10^{-5}$	1/K
Mantle thermal diffusivity	$\kappa$	$1 \times 10^{-6}$	m <sup>2</sup> /s
Mantle thermal conductivity	$k$	4	W/(m K)
Viscosity constant	$A^*$	$5.3 \times 10^{15}$	1/s
Rigidity	$\mu$	$80 \times 10^9$	Pa
Burger's vector	$B^*$	$5 \times 10^{-10}$	m
Grain size	$h$	$1 \times 10^{-3}$	m
Stress exponent	$n$	1	—
Grain size exponent	$m$	2.5	—
Activation energy	$E$	$240 \times 10^3$	J/mol
Activation volume	$V$	$5 \times 10^{-6}$	m <sup>3</sup> /mol
Equivalent pressure	$P$	$3.1 \times 10^9$	Pa
Bulk distribution coefficient	$D$	0.1	—
Mantle latent heat of melting	$L_{pm}$	$600 \times 10^3$	J/kg
Core latent heat of melting	$L$	$250 \times 10^3$	J/kg
Core gravitational energy release	$E_g$	$250 \times 10^3$	J/kg
Iron melting temperature (STP)	$T_{m0}$	1809	K
Initial crust thickness	$d_{c0}$	0	m

recognized owing to results returned from the MGS mission, in a simple, physically plausible manner. These limits include inferences of average crustal thickness [e.g., Zuber *et al.*, 2000; Kavner *et al.*, 2001] and time of crustal stabilization [Phillips *et al.*, 2001b], which are discussed in greater detail in section 4. The nominal model is by no means unique; rather, it is a description of the simplest physical processes and properties that may satisfy recent discoveries pertinent to the history of Mars. Additionally, and just as importantly, it provides a basis of comparison for exploring a fuller range of processes and material properties that may have played an important role in shaping the thermal and magmatic evolution of the planet.

[29] The nominal model consists of a fully convecting mantle in the time-dependent stagnant lid regime, with a  $Ra_i$  of the order of  $10^9$  (but obviously varying with time), and a viscosity governed by a wet, Newtonian flow law for olivine from Karato and Wu [1993]. We employ the lower, near-chondritic heat production model of Wänke and Dreibus [1994] and fractionate these elements with equal efficiency using a bulk distribution coefficient of  $D = 0.1$ . Table 3 lists the basic parameters that describe the nominal model. The model covers the time period from 4.5 Ga to the present. The initial crust is assumed to be negligible or at least to have been reassimilated into the mantle early. The mantle is assumed to be initially adiabatic with a slightly superadiabatic jump across the core-mantle boundary (CMB). Internal structure is constrained by a two-layer model that matches the normalized polar moment of inertia ( $C/MR^2 = 0.3662 \pm 0.0017$ ) [Folkner *et al.*, 1997] and bulk density of  $3933.5 \text{ kg/m}^3$  [Esposito *et al.*, 1992].

[30] Figure 2 illustrates the basic results and features of the nominal model. Mantle and CMB temperatures in Figure 2a monotonically decrease with time owing to the

loss of parent isotopes of heat-producing elements, with present-day temperatures at the base of the lithosphere near 1500 K. Figure 2b clearly depicts the growth of the crust and thermal lithosphere and the demise of an extensive layer in excess of the peridotite solidus. Total crustal thickness is  $\sim 62 \text{ km}$ , and the fractional crustal growth (fraction of maximum crust generated within the simulation) at 4 Ga is  $\sim 73\%$ . Figure 2f illustrates that pervasive partial melting ends by  $\sim 2.8 \text{ Ga}$ . Extraction of heat from the core is relatively small throughout most of the simulation, but the heat flux out of the core in Figure 2c may be quite significant during the first few hundred million years. Inner core formation is not observed in the nominal model results. Surface heat flux and the mantle contribution in Figure 2d are typical of most models. The early growth in surface heat flux is due to cooling of new crust and the presence of heat-producing elements in that crust. Crustal heat production provides the rest of the difference between the surface and mantle heat fluxes. The relative fraction of the total heat production that is generated in the crust is illustrated in Figure 2e with a total amount equal to  $\sim 26\%$  of all heat production. Average and maximum volume melt fractions as a function of time are shown in Figure 2f. The bulk crust represents an average melt fraction of  $\sim 10\%$ .

### 3.2. Effect of Variations in Heat Production

[31] Next, we step through a series of processes and material properties that may affect interpretations of thermal and crustal history models for Mars. Of paramount significance is the effect of internal heat generation. That there are two bulk composition models [Wänke and Dreibus, 1994; Lodders and Fegley, 1997], with significantly different amounts of predicted heat generation (Figure 1 and Table 2), that may be viable for Mars foreshadows significant variations in the results from the thermomagmatic models. The most significant observable effect (see Figure 3) of the different compositional models is that the higher heat production model due to LF97 predicts considerably more crust, grown at a slower rate than the nominal model based on the WD94 composition. In fact, it predicts 4 times as much crust as the nominal model and produces a smaller fraction of the total crust, by  $\sim 15\%$ , at 4 Ga. The total crustal thickness exceeds by a factor of 2 or more the upper bounds of 100–125 km placed on crustal thickness due to internal mineralogic and structural models [Kavner *et al.*, 2001] and a viscoelastic model of degree 1 crustal relaxation [Zuber *et al.*, 2000; Zhong and Zuber, 2001].

### 3.3. Effect of Latent Heat of Melting

[32] Energy consumed in the mantle and evolved in the crust owing to the latent heat of melting is a potentially significant omission from energy balance models of terrestrial planet mantles. Even if melting represents only a single percent of the mantle energy balance, when integrated over the  $>4.5 \text{ Gyr}$  lifetime of a planet, a significant amount of energy unavailable for convective, tectonic, and especially magmatic processes has been neglected.

[33] Figure 4 illustrates the substantial effect that latent heat extraction has on the system. Complete neglect of the energy of latent heat results in a crustal thickness more than twice as large as that predicted by the nominal model. This disparity is the result of enhanced mantle cooling due to latent

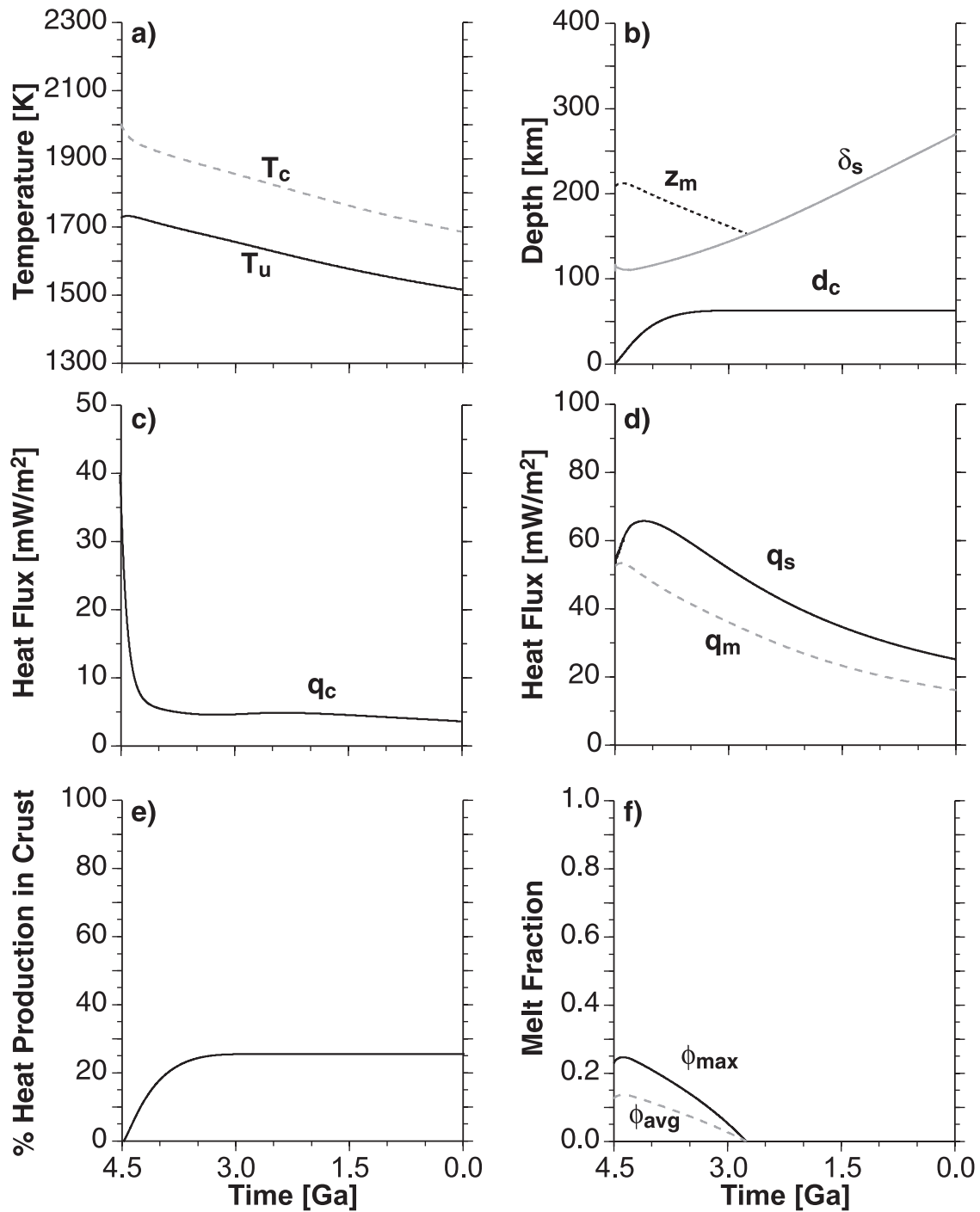


**Figure 2.** Results of the nominal model. (a) Core-mantle boundary ( $T_c$ ) and mantle-lithosphere boundary ( $T_u$ ) temperatures, (b) base of the region of partial melting ( $z_m$ ), thermal lithospheric thickness ( $\delta_s$ ), and crustal thickness ( $d_c$ ), (c) heat flux out of the core at the core-mantle boundary, (d) surface heat flux ( $q_s$ ) and heat flux into the base of the lithosphere ( $q_m$ ), (e) fraction of heat production in the crust, (f) maximum and average volumetric melt fractions as a function of time.

heat in the nominal model. Owing to the gradient ( $\partial T/\partial P$ ) of the peridotite solidus, small decrements of temperature can lead to significant decrements in melt fraction and maximum melt depth. The nonlinear variation in crustal thickness with the latent heat of melting is likely principally due to the highly nonlinear variation of melt fraction with temperature and the peridotite solidus [e.g., McKenzie and Bickle, 1988; Zhang and Herzberg, 1994], especially where

exhaustion of clinopyroxene has a significant effect on these quantities [e.g., Hirschmann *et al.*, 1999]. Fractional crustal growth is similar, within a couple percent, to nominal model results regardless of the value of latent heat of melting.

### 3.4. Effect of Stagnant Lid Convective Regime

[34] As there are two basic subtypes of convection in the stagnant lid regime, we investigate the relative effects that

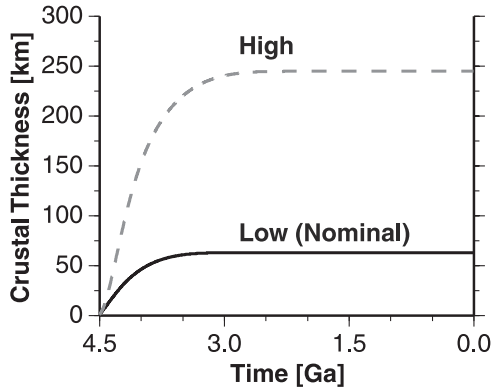


**Figure 3.** Crustal thickness as a function of time and heat production. The high heat production model of *Lodders and Fegley* [1997] produces 250 km of crust compared to the 62 km of the nominal model based on the *Wänke and Dreibus* [1994] composition.

they have on the thermomagmatic evolution of Mars. Steady stagnant lid convection is observed in numerical experiments [e.g., *Reese et al.*, 1999] and may be representative of convection where well-developed, equidimensional convective cells are present. The more time-dependent convection results are well predicted by analytic theory [*Solomatov*, 1995] and numerical exercises at high Rayleigh numbers [e.g., *Solomatov and Moresi*, 2000]. In addition, steady stagnant lid convection has been previously applied to models of Mars [*Reese et al.*, 1999], and hence a comparison of their effects is appropriate.

[35] The parameters that describe the two regimes (listed in Table 1) indicate that the time-dependent regime is more efficient at transferring heat than the steady stagnant lid regime. The difference in efficiency is governed predominantly by the exponential constant  $c$  for the Rayleigh number. For example, the steady value for a Newtonian,  $n = 1$ , fluid is one fifth, which is less than the time-dependent value of one third. Plainly stated, less efficient cooling leads to a longer period of time over which temperatures in the upper mantle may be supersolidus, leading in

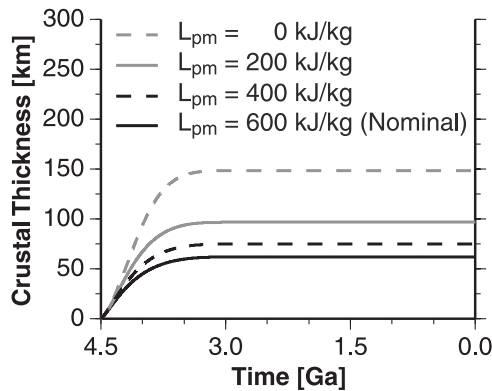


**Figure 4.** Crustal thickness as a function of time and latent heat of melting. Inclusion of the latent heat of melting results in more than a factor of 2 reduction in predicted crustal thickness compared to models that do not include latent heat.

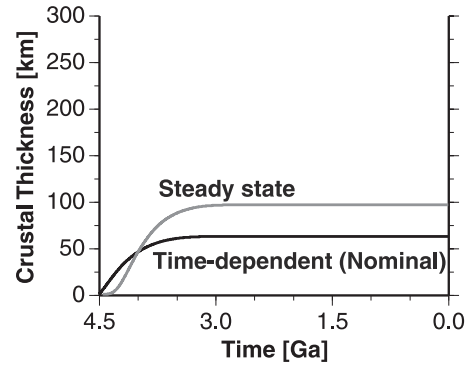


**Figure 5.** Crustal thickness as a function of time and stagnant lid convective regime. Steady state stagnant lid convection is less efficient than the time-dependent mode and results in almost 50% more crust than the nominal model.

turn to a thicker predicted crust. Figure 5 demonstrates this point where total crustal production calculated in the steady model is enhanced relative to the nominal model in the time-dependent regime. The less efficient steady mode of stagnant lid convection results in almost 50% more crust than the nominal model.

### 3.5. Effect of Non-Newtonian Viscosity

[36] Flow of mantle rocks over geologic timescales may be analogous to Newtonian or non-Newtonian fluids. Dislocation (non-Newtonian) creep mechanisms may play a significant role in mantle flow and deformation within the Earth (review by *Karato and Wu* [1993]). In order to investigate the role that non-Newtonian viscosity may have on the evolution of the Martian mantle, we must first modify the Rayleigh number relation for general  $n$  [*Reese et al.*, 1999; *Solomatov and Moresi*, 2000]:

$$Ra = \frac{g\alpha(\Delta T)d^{(n+2)/n}}{A^{1/n}\kappa^{1/n}\exp\left(\frac{E+PV}{nRT}\right)}. \quad (13)$$

The  $A$  and exponential terms represent the viscosity term in equation (3). The term  $A$  is a combined pre-exponential constant given by

$$A = \frac{\mu^n}{3^{(n+1)/2}A^*} \left(\frac{h}{B^*}\right)^m. \quad (14)$$

Dislocation creep is essentially grain-size independent, so  $m = 0$ . Dislocation creep of wet olivine has an  $A^* = 2.0 \times 10^{18} \text{ s}^{-1}$ ,  $n = 3$ , and  $E = 430 \text{ kJ/kg}$ . Furthermore, we use an intermediate value of activation volume of  $V = 15 \times 10^{-6} \text{ m}^3/\text{mol}$  [*Karato and Wu*, 1993].

[37] Figure 6 demonstrates that dislocation creep results in a thicker average crustal thickness compared to the nominal model with diffusion creep of wet olivine. The activation enthalpy plays a strong role in this result, which is affected by the large activation volume for dislocation creep (by a factor of  $\sim 3$ ) relative to diffusion creep. The decreased temperature dependence of viscosity in the dislocation regime may play the dominant role, because for low to moderate driving stresses diffusion creep may

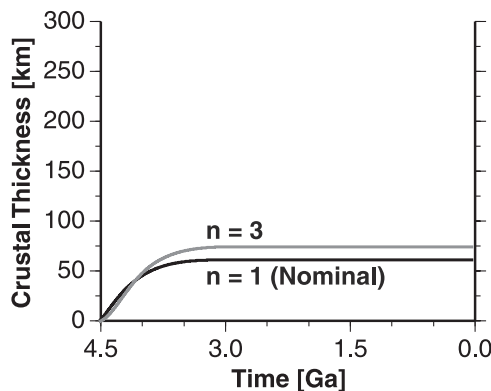


**Figure 6.** Crustal thickness as a function of time for Newtonian and non-Newtonian creep of wet olivine. Non-Newtonian viscosity results in slightly more crustal production owing to its slightly lower convective efficiency, consistent with the results of *Solomatov and Moresi* [2000].

provide a lower viscosity. However, uncertainty concerning the grain size for diffusion creep and the activation volume for dislocation creep ( $V = 10 \times 10^{-6} - 20 \times 10^{-6} \text{ m}^3/\text{mol}$ ) does not allow us to rule out the possibility that the results are not as different as Figure 6 might suggest. While dislocation creep may be a dominant mechanism of mantle flow and deformation, its effect on the efficiency of well-developed convection is not necessarily the most significant effect.

### 3.6. Effect of Differentiation of Heat Producers to the Crust

[38] Incompatible elements, such as the predominant heat producers, tend to preferentially differentiate into the crust owing to their affinity for melt relative to solid materials. The result is that there are higher concentrations of heat-producing elements in the crust than in the mantle. Crustal sequestration of heat-producing elements has two main consequences: first, it reduces the driving energy for convection within the mantle, and second, it results in a warmer (thinner) lithosphere than would be expected without crustal heat production. Bulk distribution coefficients between zero and one are representative of incompatible elements whose behavior may be described by a batch melting process [e.g., *Brownlow*, 1996].

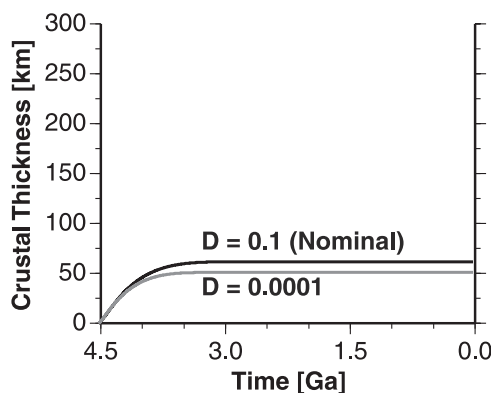


**Figure 7.** Crustal thickness as a function of time and batch melting bulk distribution coefficient.

[39] Figure 7 illustrates the effect of two different distribution coefficients for strongly incompatible elements. The nominal bulk distribution coefficient,  $D = 0.1$ , represents significant solid-liquid incompatibility. However, to test the sensitivity of the system to the possibility of even stronger fractionation of heat producers into the crust, we have chosen a bulk distribution coefficient 3 orders of magnitude smaller ( $D = 0.0001$ ) for comparison. A model with such highly incompatible heat producers results in only  $\sim 10 \text{ km}$  ( $\sim 15\%$ ) less average crust created than in the nominal model. This result is due to extraction of  $\sim 10\%$  more of the heat producers from the mantle than the nominal model (see Figure 2e). Removal of additional radiogenic isotopes from the mantle allows for the interior to cool more, because there is less heat being generated, and hence less heat that must be removed from the mantle. Because the mantle can cool more quickly in this mode, the internal temperatures drop and the lithosphere grows more (relative to the nominal model) and pervasive melting is shut off more quickly. The relatively small difference in predicted crustal thickness for such a large difference in fractionation efficiency suggests that the nominal model captures well the effects of differentiation of heat producers due to a batch mode of magma generation and extraction.

### 3.7. Effect of Melt Productivity

[40] The characterization and understanding of melt productivity in the mantle at the microscale and macroscale are areas of intense interest because of their obvious implications for a host of problems, including those related to terrestrial mid-ocean ridge and island arc regions [e.g., *Hirth and Kohlstedt*, 1996; *Asimow and Stolper*, 1999] in addition to the coupled thermal and crustal evolution of Mars. Our nominal melt production model is limited to the case of equal upwelling and lateral velocities within the region of melt. It is possible, however, that lateral viscosity variations due to temperature and even the effects of melting may induce magma focusing, which could limit the total productivity. We can examine the results of this case in a simple manner by imposing a focusing factor between 0 and 1 where 1 implies no focusing (nominal model) and 0 has no melt production. It is conceivable that magma production could be as much as 50% lower than expressed in the nominal model. Figure 8 illustrates quantitatively the intuitive

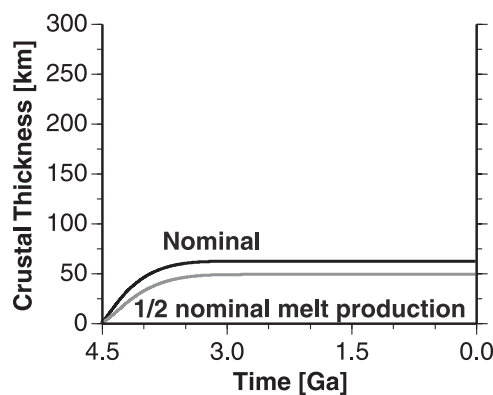


**Figure 8.** Crustal thickness as a function of time and melt production. A 50% reduction in melt production results in only 16 km less predicted crust than the nominal model.

tively obvious effect, lower melt production results in less crust. The interesting point is that a 50% reduction in the magma production results in only  $\sim 15$  km ( $\sim 22\%$ ) less total crust than the nominal model. The reduction of melt production by a factor of 2 has been partially offset by the lower cooling rates owing to less extraction of latent heat and heat-producing elements relative to the nominal model.

### 3.8. Effect of Variable Thermal Conductivity

[41] Thermal conductivity is a key parameter in description of heat transfer via conduction. Canonically, it is assumed to have a constant value of  $\sim 4$  W/(m K) [e.g., *Turcotte and Schubert, 1982*] in models of heat transfer in lithospheric and mantle materials. Recently, *Hofmeister [1999]* presented a model based on phonon lifetimes for how thermal conductivity varies with temperature and pressure that appears to match available data for a range of minerals from salts to silicates. An important aspect of this model, as well as previous models of the temperature-dependence of conductivity [*Schatz and Simmons, 1972*], is that conductivity generally decreases with increasing temperature (pressure and radiative contributions have the opposite effect). Temperature dependence is the most significant effect in the lithosphere and upper mantle and results in a lower “effective” conductivity and hence thinner lithospheres [*Hofmeister, 1999*]. While some work has begun on the effect that variable conductivity has on mantle convection [*van den Berg et al., 2001*], the efficiency of the heat transfer process seems most dependent on the radiative contribution in the lower mantle (for the Earth) for the variable conductivity case. Because a lower mantle is principally absent in our models of Mars, and represents at most a thin layer in other structural models [*Bertka and Fei, 1997; Kavner et al., 2001*], our results should not be affected by the potentially enhanced efficacy of heat transfer due to radiative effects. However, the implication for the thickness of the lithosphere is that it should be thinner with variable conductivity as opposed to constant conductivity.

[42] A comparison of results for a model with variable conductivity (using parameters for olivine [*Hofmeister, 1999*]) governing conduction through the lithosphere and the nominal model with constant conductivity is shown in Figure 9. Indeed, significantly more crust ( $\sim 50\%$ ) is gen-

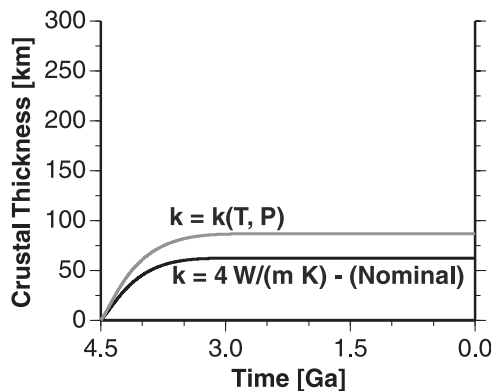


**Figure 9.** Crustal thickness as a function of time for constant and variable thermal conductivity. Variable conductivity leads to a 50% increase in predicted crustal thickness relative to the nominal model.

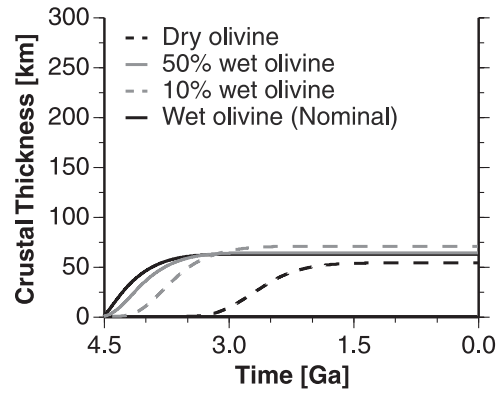


**Figure 10.** Crustal thickness as a function of time for constant and water saturation. Decreasing water content strengthens the mantle and leads to slower crustal growth rates relative to the nominal model.

erated relative to the nominal model owing to a thinner lithosphere. The thinner lithosphere implies that the melt channel is relatively thicker in the variable conductivity model, and hence there is greater magma production.

### 3.9. Effect of Mantle Water Content

[43] Water is a principal agent limiting the viscous strength of rocks [e.g., *Chopra and Patterson, 1984; Mackwell et al., 1985; Karato et al., 1986; Karato and Wu, 1993; Mackwell et al., 1998; Hirth and Kohlstedt, 1996; Mei and Kohlstedt, 2000a, 2000b*]. Rocks saturated in water are considerably weaker than dry ones. Weak (wet) rheologies convect more easily and hence transfer heat more efficiently than strong (dry) rheologies. Thus a system with a wet rheology will cool more quickly than a dry system. In addition, an important physical corollary is that the wet system will have a thinner lithosphere at a given temperature contrast compared to the dry system. A dry mantle will have a thinner melt channel than a wet mantle for the same internal temperature.

[44] Recent work on the variation of viscosity with water content in olivine [*Mei and Kohlstedt, 2000a, 2000b*] has established that there is a roughly linear to sublinear dependence of strain rate on water fugacity. This dependence reveals that even moderate levels of water saturation in the mantle may significantly weaken the rheology relative to one that is completely dry. Using this result as a guide and the wet and dry rheologies of *Karato and Wu [1993]* as end-members, we have investigated the general effects that water content has on our models. We constructed two simple, intermediate cases where we set the viscosity to be 10 and 50% of the way between dry and wet to simulate similar levels of water saturation in the mantle. The general result is that decreasing water content leads to significantly slower growth rates as depicted in Figure 10. The trend is easily understood; for a given initial temperature the melt channel will be thinner in a planet with relatively less water. This effect is due to the general increase of viscosity with decreasing water content. All other aspects being equal, the increase in viscosity leads to a decrease in Rayleigh number, which implies a thicker thermal lithosphere (the upper limit of the melt channel). The most dramatic result is clearly the

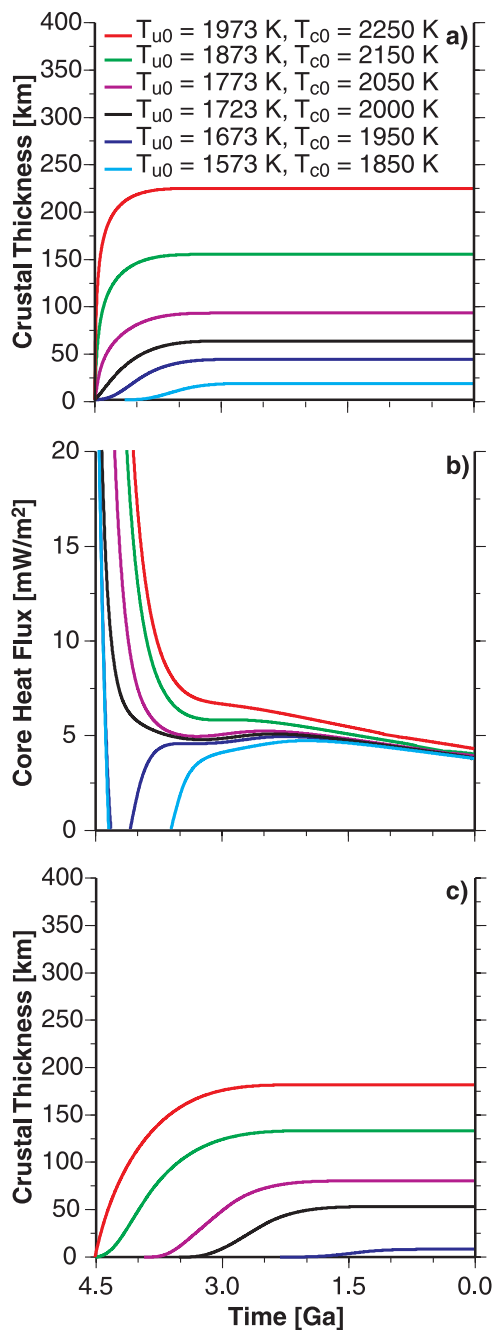


**Figure 11.** (a) Crustal thickness as a function of time and initial thermal state for wet olivine, (b) core heat flux as a function of time for the same conditions in Figure 11a, and (c) same as Figure 11a but for dry olivine.

effect on growth rate; the dry model has virtually no crust before 3 Ga in contrast to the wet or even 50% wet models.

### 3.10. Effect of Initial Temperature

[45] Internal mantle temperature is the key control on both convection and melting in terrestrial planets. The early thermal state of terrestrial planets is complex and dependent on processes such as accretion, core formation, large impacts, and magma oceans [e.g., *Sleep, 2000*]. For example, core formation on Mars should have raised the internal

temperature of the body by 300 K (compared to more than 2000 K for the Earth) [*Solomon, 1979*]. Rather than include additional free parameters related to such processes, we simply vary the initial temperatures systematically to quantify how our results are affected. There are three primary impacts that initial temperature has on the system. First, the starting thermal state controls the initial melting state of the system, including the fraction of partial melt available and the depth of the melt channel. The larger each of these quantities is, the greater the amount of crust that can be created more rapidly. The rate at which crust is created is strongly controlled by the strength of the mantle, as demonstrated in the previous section. Second, hotter rocks flow more easily and hence supply material to the melt channel at a faster rate than cooler material. Higher temperatures imply thinner thermal lithospheres, which in turn imply thicker melt channels. Third, the potential for an internally driven magnetic field early in Mars' history [*Acuña et al., 1999*] is a function of the core heat flux [e.g., *Stevenson et al., 1983; Schubert and Spohn, 1990*], which is controlled by the thermal conditions.

[46] We have systematically varied the initial upper mantle ( $T_{u0}$ ) and core-mantle boundary ( $T_{c0}$ ) temperatures over a range of 400 K. In addition, all models start with a fixed contrast between the upper mantle and the CMB of 277 K, which accounts for an adiabatic mantle and a relatively small, superadiabatic temperature contrast across the CMB. Figures 11a and 11b illustrate how crustal thickness and the flow of heat out of the core varies with the initial thermal conditions; the solid black line denotes the nominal model as in previous figures. Initial mantle temperatures in the range of 1700–1800 K bound reasonable crustal thicknesses of  $\sim 50$ –100 km. In addition, high initial temperatures lead to faster crustal growth rates compared to models that are initially cooler. Figure 11c illustrates the same range of initial thermal states, but for the dry olivine end-member. It is obvious that increased initial mantle temperatures with a dry olivine rheology when compared to the nominal model do not lead simultaneously to fast crustal growth rates and moderate total crustal thicknesses, as might be the expected trade-off.

[47] The initial thermal state influences strongly both the early cooling of the core and the potential for inner core solidification if the core has remained liquid throughout most (or all) of its history. The length of time that the early heat flux could have remained above that conducted along a core adiabat depends on how much it must cool to reach a state that is in lockstep with mantle cooling; the higher the initial temperatures, the longer period that rapid cooling dominates. Figure 11b demonstrates that for initial conditions with  $T_{u0}$  much less than 1700 K it is possible that the core may go through a period of heating rather than cooling. Such a possibility has been previously proposed for Mars [*Nimmo and Stevenson, 2000*] as a result of a switch in convective regime from early plate tectonics to stagnant lid. While not modeled here, it is conceivable that such a process occurred at or before the beginning of our models, which start at 4.5 Ga.

### 3.11. Effect of an Enriched Primordial Crust

[48] Geochemical evidence suggests that Mars experienced an early silicate differentiation event that has

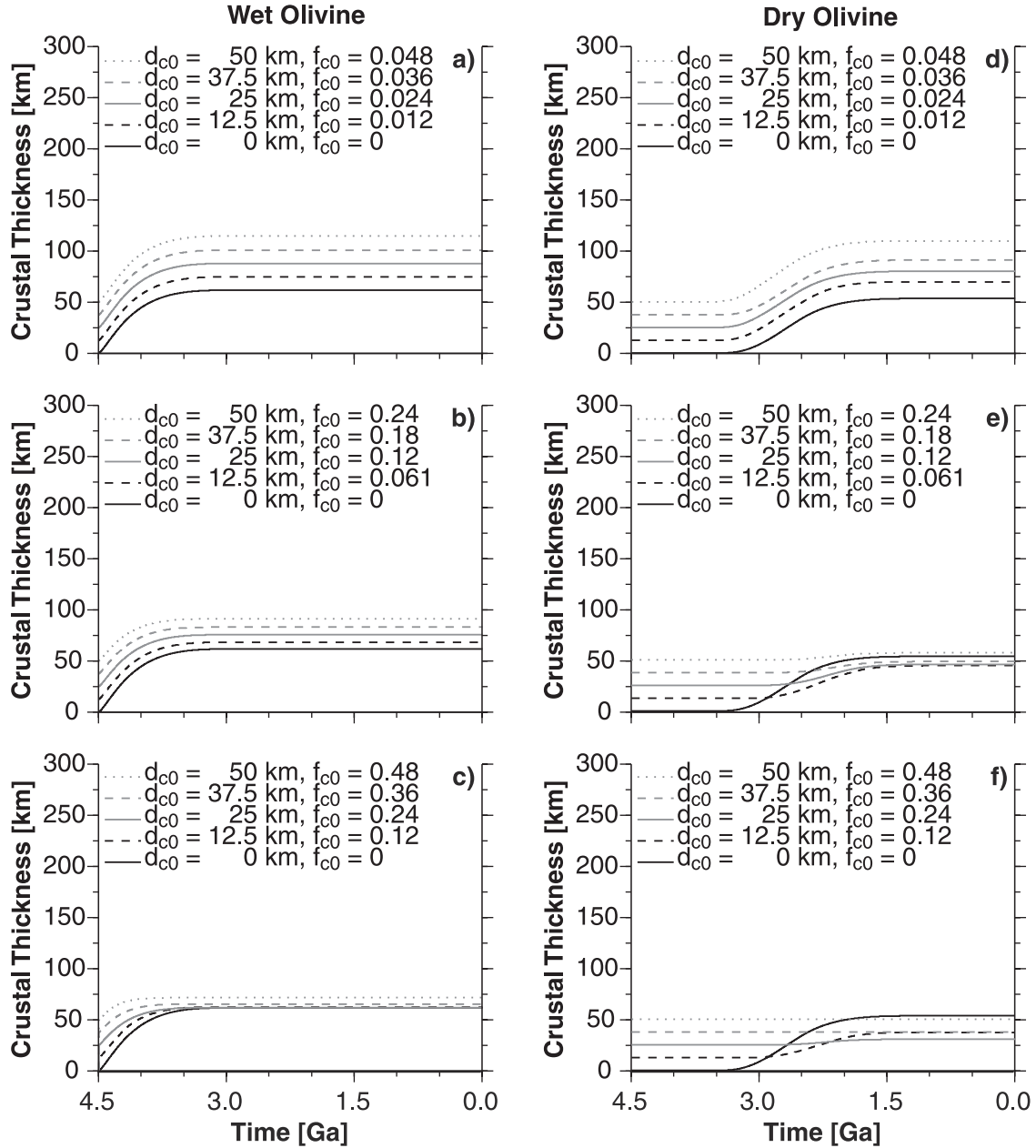


**Figure 12.** Crustal thickness as a function of time, initial crustal thickness, enrichment of heat-producing elements, and mantle rheology. Figures 12a–12c are for wet olivine mantle rheology, and Figures 12d–12f are for dry olivine mantle rheology. In Figures 12a and 12d, crustal enrichment is  $1 \times$  primitive Martian mantle (PMM). In Figures 12b and 12e, crustal enrichment is  $5 \times$  PMM. In Figures 12c and 12f, crustal enrichment is  $10 \times$  PMM. Initial crustal thickness ( $d_{c0}$ ) varies from 0 to 50 km, and  $f_{c0}$  is the initial fraction of all heat-producing elements residing in the crust.

influenced the isotopic character of the SNC meteorites [e.g., Harper et al., 1995; Lee and Halliday, 1997; Blichert-Toft et al., 1999]. Such a process would have produced a primordial crust that would have influenced the subsequent evolution of the planet and represents some unknown fraction of the present-day crust. A consequence of a primordial crust is early sequestration of heat-producing elements, potentially reducing later mantle melting and crustal additions. In order to quantify the effects of a primary crust on the evolution of the planet, we have varied both its thickness and heat-producing element enrichment in our models. We have

investigated three cases of initial crustal heat producer enrichment of 1, 5, and 10 times the concentration of the WD94 estimate for the primitive Martian mantle (Table 1). In addition, we have considered initial crustal thicknesses up to 50 km and the effects of wet and dry rheologies.

[49] Figure 12 illustrates how evolution of the crust varies for different primary crustal thicknesses, concentration of heat-producing elements, and mantle strengths. Figure 12a–12c for a wet mantle and Figure 12d–12f for a dry mantle both display the intuitively expected result that increasing enrichment of the primordial crust leads to decreasing

subsequent new crustal additions to the crust. It is clear that a primary crust with a heat-producing element content equivalent to the primitive Martian mantle has little effect on the system other than to increase the total amount of crust generated relative to the nominal case with zero initial crust. Crustal enrichments of 5–10 times the primitive concentration do trend toward limiting total crustal thickness and the time over which substantial crustal additions are made. While models with a wet Martian mantle, with and without a primordial crust, tend to complete most of their crustal additions by 4 Ga, those with a dry mantle can experience the onset of major crustal additions after 3 Ga, and in the case of significant crustal enrichment (Figure 12e–12f) may exhibit little to no additions to the primary crust. In addition, the combination of a dry mantle and extreme crustal sequestration [e.g., *McLennan*, 2001] of heat-producing elements (e.g., the case with  $d_{c0} = 50$  km and 48% of the heat producers in the primary crust in Figure 12f) leads to thick thermal lithospheres in excess of 500–600 km between 4.5 and 4 Ga.

## 4. Discussion

### 4.1. Potential Constraints and the Nominal Model

[50] The thermal and magmatic evolution of Mars is the result of a complex set of processes acting in concert. Limitations on this history are few and only partially constrained. The most intriguing and potentially useful geophysical limits on the problem relate to the growth history of the crust, thickness of the crust, and the existence of an internally generated magnetic field. Recent geophysical [*Zuber et al.*, 2000] and mineral physical [*Kavner et al.*, 2001] work has placed bounds on average crustal thickness of ~50–125 km. *Zuber et al.* [2000] used MGS gravity and topography data to invert for crustal thickness variations assuming that the whole Bouguer gravity anomaly could be accommodated by deflection of a Moho between a constant density crust and mantle. If lateral variations in crustal density and mass anomalies within the mantle represent a negligible fraction of the Bouguer field, then by requiring that there can be no regions of negative crustal thickness, it is possible to place a lower bound on average crustal thickness. *Zuber et al.* [2000] found that an average crustal thickness of 50 km satisfied this case. In addition, by using the viscoelastic model of *Zhong and Zuber* [2000], they argued that the degree one (north pole to south pole) crustal thickness variation could be maintained over time if the average crustal thickness was closer to 50 km but not if it was near the 100–250 km range previously suggested by *Sohl and Spohn* [1997]. *Kavner et al.* [2001] place an upper bound on crustal thickness of 125 km using the normalized polar moment of inertia (to  $\pm 4\sigma$ ) and new determinations for the density of FeS under conditions likely prevalent in the Martian core. Recent geochemical work using a neodymium mass balance model has suggested a crustal thickness in the range of 10–45 km with a most probable thickness of 20–30 km; however, this is more likely consistent with an early developed crust rather than the total volume [*Norman*, 1999, 2002].

[51] Placing constraints on crustal growth rate seems a difficult prospect, but Mars has some unique properties that may provide at least two points on the crustal growth curve.

*Phillips et al.* [2001b] demonstrated that in addition to rotational flattening and the pole-to-pole slope [*Smith et al.*, 1999], the long-wavelength gravity and topography of Mars are dominated by a membrane response of the lithosphere to the load of the Tharsis province. Mapping of the Margaritifer Sinus region by *Hynek and Phillips* [2001] suggested that early fluvial activity on Mars was structurally influenced by the presence of the trough between Tharsis and Arabia Terra. A comparison of valley network (which are generally Noachian in age) downstream directions with that predicted by the Tharsis-dominated model indicates that Tharsis must have been in place by the end of the Noachian [*Phillips et al.*, 2001b]. Also consistent with this idea are predictions of stress and strain from models of lithospheric flexure in the Tharsis province constrained by present-day gravity and topography. These predictions correlate with the displacement and orientation of faults at the peak of faulting in the early and middle Noachian in the circum-Tharsis region [*Banerdt and Golombek*, 2000]. These results suggest that a bulk of the Tharsis load must have been emplaced early, likely by the late Noachian-early Hesperian boundary. The idea of early Tharsis emplacement in turn implies that the crust was predominantly stabilized by this time as well. Therefore a significant fraction of the crust must have been emplaced by ~4 Ga or earlier.

[52] *Zuber et al.* [2000], in addition to deriving crustal thickness variations, estimated the equivalent elastic plate thickness required to support several surface loads flexurally, like the Tharsis montes and Hellas. Estimates of elastic thickness and plate curvature were then converted to heat flux using an elastic-plastic plate model [*McNutt*, 1984; *Solomon and Head*, 1990]. Derived elastic plate thicknesses and heat fluxes are assumed to be representative of the time of loading. Results from an elastoviscoplastic model of lithospheric deformation suggest that for a uniformly cooling plate this “frozen in” paleoflexure is reasonable, although estimates of effective elastic plate thickness from present-day observations may be underestimated by 10% or more in areas affected by anomalously high temperatures (e.g., volcanic magma conduits) [*Albert and Phillips*, 2000]. *Zuber et al.* [2000] noted a discrepancy between their estimates of heat flux derived in this manner and earlier thermal evolution models [i.e., *Schubert and Spohn*, 1990], especially for ancient, southern, Noachian terrains. They interpreted their derived lower than average expected heat flows for the southern hemisphere to be suggestive of higher than average heat flows elsewhere in the Noachian, such as the northern plains, which has been suggested as potential locus of ancient plate tectonics. Such an interpretation, however, may be unwarranted. As noted above, the models of *Schubert and Spohn* [1990] and *Schubert et al.* [1992] utilize a high heat production model that is inconsistent with inferred crustal thicknesses and crustal growth rates for Mars. A lower heat production model like that due to *Wänke and Dreibus* [1994] brings the results into much closer agreement, potentially abrogating the need to invoke northern hemisphere plate tectonics to explain heat fluxes in the Noachian era.

[53] We have two basic potential constraints on the thermal and crustal formation history of Mars. The strongest constraint is the limit on average crustal thickness of ~50–125 km. In addition, the crust was likely predominantly

emplaced by  $\sim 4$  Ga. The results of the nominal model generally do the best job of satisfying these constraints under a simple set of conditions. The fact that the crust is 73% emplaced by 4 Ga (and almost >95% by 3.5 Ga, the lower bound of the late Noachian-early Hesperian boundary [i.e., *Tanaka et al.*, 1992]) with only 62 km of total crust created is a strong aspect of the model. Mantle temperatures are reasonable, and pervasive mantle melting shuts down by 2.8 Ga. Average melt fractions of 10% or less are also reasonable and are representative of much of the early magma generation in the nominal model. Melt fractions of the level may be in accord with inferences of partial melt fractions of 2–8%, which are consistent with light rare earth element abundances [*Norman*, 1999].

#### 4.2. Energy of Heat Production and Latent Heat of Melting

[54] It is clear within the context of our modeling that heat generation within Mars cannot be significantly greater than the *Wänke and Dreibus* [1994] composition implies. The factor of 3 greater abundance of potassium in the *Lodders and Fegley* [1997] model leads to unreasonable crustal thickness estimates almost 4 times greater than the nominal model. Unless some early differentiation process sequestered large amounts of heat-producing elements in the early crust (especially K), it seems unlikely that compositional models for Mars with greater than chondritic abundances of K, U, and Th are representative of the planet's bulk composition. In fact, analysis of shergottites suggests that they have an average potassium content that is not enriched relative to chondritic [e.g., *Ruzicka et al.*, 2001], which is consistent with a bulk composition that is not enriched relative to chondritic either. In addition, even this extreme case will be limited by the fact that increased crustal heat production leads to a reduction in the effective degree one crustal thickness variation that may be supported over time because the crust will be relatively hotter and more likely to flow in this situation. However, such a high concentration of K may not be consistent with surface measurements [e.g., *Banin et al.*, 1992].

[55] Energetically speaking, melt generation and extraction are relatively small contributors to the entire history of a planet over 4.5 Gyr. Through the process of including the latent heat of melting in the mantle and lithospheric energy balances we must necessarily calculate the amount of energy related to (consumed in the mantle and evolved in the crust) the latent heat of melting. If we integrate the total energy lost through the surface of the planet through time, we also know the total amount of energy lost through the surface (of which some fraction is related to the latent heat of melting). In fact, energy lost in the nominal model related to the latent heat of melting is less than 3% of the total energy budget over 4.5 Gyr. However, the early melting is quite massive and represents more than 13% of the energy budget between 4.5 and 4 Ga, although by 4 Ga the energy related to latent heat being lost by the planet is only 4%. Quite simply, this means that while the energy involved in melting is a small fraction of the total planetary energy budget, it is nonnegligible.

[56] It is important to note, however, that our models cannot completely represent the physical and energetic consequences of melting and crustal generation within a

convecting system. We are not aware of any such scaling relationships within the literature, and the hurdles to full understanding of the problem are significant. Melt generation and extraction alter, at least, the viscosity, density, and thermal regime of the system. The viscous strength of partially molten systems, while a topic of intense interest (review by *Kohlstedt and Zimmerman* [1996]) may yet be lacking an adequate description that captures effects of a solid-liquid system as well as the dehydration of solids during melting [*Hirth and Kohlstedt*, 1996]. In addition, numerical work has begun to shed a little light on the dynamics of a system undergoing partial melting [*Ogawa*, 1993; *DeSmet et al.*, 1999] but has yet to elucidate consequences for the efficiency of the convective system. In the absence of such physical knowledge we are left simply with the option of estimating the purely energetic effects due to the thermodynamics of melting.

#### 4.3. Model Sensitivity to Additional Processes

[57] Convection in terrestrial planet mantles is a complex process. Modeling coupled convection-melting systems is an important step in trying to understand how planetary mantles may work. The nominal model was designed to be simple so that we might gain some physical insight about the system. In order to outline the sensitivity of crustal production in a coupled convection-melting system we investigated the effects of a range of physical processes. Mantle convection may be either steady [e.g., *Solomatov and Moresi*, 1996; *Reese et al.*, 1999] or time-dependent [e.g., *Dumoulin et al.*, 1999; *Solomatov and Moresi*, 2000]. In a relative sense, time-dependent convection is more efficient at transferring heat, and such models result in lower crustal thicknesses and higher fractional crustal growth rates than the steady models.

[58] Rheology plays a primary role in the evolution of planetary crusts and mantles. Deformation of the Earth's upper mantle is believed to be dominated by nonlinear, dislocation creep [*Karato and Wu*, 1993]. However, given the uncertainties in grain size and activation volumes, models of time-dependent stagnant lid convection beneath the Earth's oceanic lithosphere using dislocation and diffusion viscosity are indistinguishable [*Solomatov and Moresi*, 2000]. This result suggests that distinguishing among diffusion and dislocation creep mechanism in the long-term evolution of planetary mantles is quite difficult indeed.

[59] The roles of variable thermal conductivity and melt productivity are potentially more significant. The role that temperature- and pressure-dependent conductivity plays in the long-term thermal evolution of the crust and lithosphere is still uncertain. However, the general decrease in conductivity with temperature supports the idea that lithospheric thickness predictions based on constant conductivity will be overestimates. Magma generation is strongly dependent on melt channel thickness, which is a function of lithospheric thickness, and variable conductivity may imply greater crustal production than the nominal model suggests. As crustal production is directly related to the flux of material through the melt channel (see equation (9)), anything that might focus material or slow the material below the interior convecting velocity such as a viscosity increase due to dehydration and melting would reduce the predicted magma generation. The highly

focused upwelling of material at terrestrial mid-ocean ridges is an example of such an effect (although not entirely analogous owing to the lack of spreading centers in one-plate planets). Such a reduction in melt productivity is plausible and will indeed reduce the amount of crust generated, potentially offsetting any increase in crustal production that variable conductivity may induce.

#### 4.4. Water

[60] The role of water on the viscous strength of mantle materials is more dramatic, as even small amounts of water may sufficiently weaken the material [Karato and Wu, 1993; Hirth and Kohlstedt, 1996; Mei and Kohlstedt, 2000a, 2000b]. Furthermore, a wet olivine rheology provides the best fit for the temperature and heat flux for small-scale (time-dependent stagnant lid) convection beneath the Earth's oceanic lithosphere [Solomatov and Moresi, 2000]. Data for the solubility of water in olivine [Hirth and Kohlstedt, 1996; Kohlstedt et al., 1996] indicate that a mere 20 ppm of water in olivine is 40% saturated at 1 GPa ( $\sim 100$  km depth on Mars) and is  $\sim 10\%$  saturated at 3 GPa ( $\sim 300$  km). Water is  $\sim 90\%$  saturated in olivine at 1 GPa and  $\sim 25\%$  saturated at 3 GPa for a concentration of 50 ppm. Figure 10 clearly illustrates that even 10% saturation of water in olivine results in a considerably faster fractional crustal growth rate than purely dry olivine. Water plays a singular role in the thermal and crustal evolution of the planet.

[61] Water, it seems, in addition to being an important agent in surface evolution on Mars [Carr, 1996], is a key ingredient in the planet's internal evolution as well. However, water is an incompatible constituent in a solid-melt system. Melting leads to dehydration of residual mantle. A discontinuity within the Earth's mantle at 60–80 km depth may be a result of such dehydration due to partial melting [e.g., Hirth and Kohlstedt, 1996]. Within the Earth, water is recycled, albeit very inefficiently, via crust and lithosphere recycling at subduction zones. In the absence of whole-scale lithospheric recycling, water fluxed through the melt channel is likely lost permanently from the mantle. This raises the question, Will large-scale crustal formation and mantle melting lead to significant additional degassing of the mantle? The simplest way to address this question is to calculate how much water is fluxed through the melt system and extracted. Assuming perfect extraction of all water that enters the melt channel provides an upper bound to the problem. Using the magma generation model we have already described, we can easily calculate the water lost from a mantle with a homogenous water concentration. In order to capture a wide range of possibilities we have calculated fractional mantle water loss for all results presented in Figure 11a. Figure 13 demonstrates dramatically that devolatilization of the mantle after the initial phase of accretion and degassing is quite small. At least 90–95% of all water left in the Martian mantle after the initial degassing [e.g., Hunten, 1993] should still be there today.

[62] Water is a dominant factor in the strength of mantle rocks, modest concentrations of water (even 20–50 ppm) imply moderate to high degrees of water saturation in olivine, and more than 90% of the water in Mars' mantle at 4.5 Ga should still be there today. Does Mars have enough mantle water in order for the mantle to have at

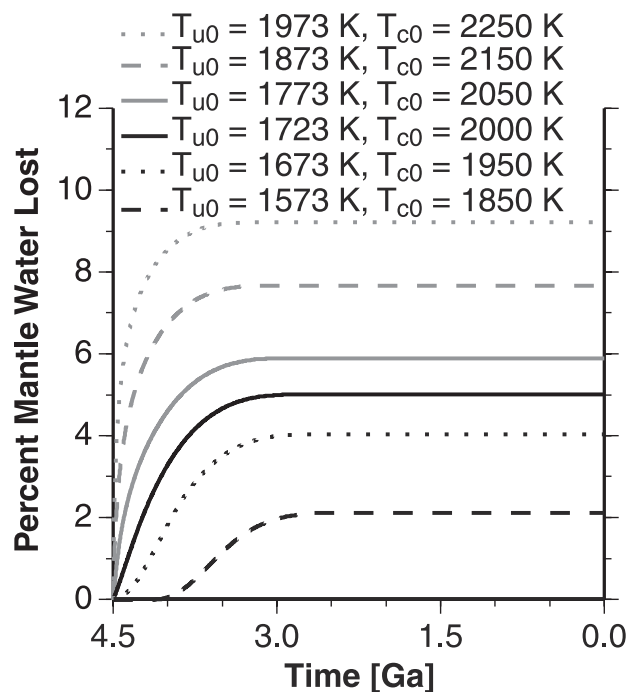


**Figure 13.** Fractional mantle water loss as a function of time for the same set of conditions in Figure 11. The maximum amount of water that may be extracted from the mantle due to postaccretion and initial degassing processes is less than 5–10% of the initial amount.

least a moderately weak rheology? Estimates for the amount of water in the Martian mantle, principally based on study of the Chassigny meteorite (a dunite), range from a minimum of 1 ppm [Mysen et al., 1998] to a maximum of 1000 ppm [Johnson et al., 1991]. More recently, McSween et al. [2001] have estimated that water contents in the shergottite ( $\sim 170$  Ma) source magma may have been as high as 1.8 wt %, lending credence to the idea that the water content of the Martian mantle may be quite high, and that significant water was still available to recent magmatic activity. However, the inferred source depth of  $\sim 5$  km indicates that a meteoric origin for the magmatic water cannot be ruled out. Interestingly enough, the Wänke and Dreibus [1994] bulk composition model suggests that  $\sim 36$  ppm of water may be available in the Martian mantle. While a 4 order of magnitude range of estimates for mantle water concentration exists, abundances at the 40 ppm or greater level seem most likely. Such abundances in bulk composition calculations suggest that sufficient water exists within the Martian upper mantle to support the conclusion that a significantly wet rheology is an appropriate choice to match constraints on Mars' thermal and crustal evolution.

[63] Furthermore, we can estimate in a similar manner the total amount of water that might be delivered to the crust and surface owing to magma generation in a similar manner. If the mantle contains 36 ppm water by mass, there would be an equivalent global surface layer of extracted water 6.4 m thick ( $\sim 9.3 \times 10^{14} \text{ m}^3$ ) for the nominal model. On average, this volume represents  $\sim 100$  ppm of water in emplaced crust. Fractional crystallization of magma would imply far greater water concentrations delivered to the surface and atmosphere by surface volcanism. Crustal

genesis and volcanism on Mars may provide a significant source of water available to influence the early climate and surface modification of the planet. Traditional arguments for a wet Mars include landform morphologies reminiscent of running water like valley networks and outflow channels [Carr, 1996] and the deuterium-hydrogen fractionation observed in Martian meteorites [e.g., Leshin, 2000]; however, the necessity of a wet mantle and the rapid development of the crust and concurrent extraction of water from the mantle provide an additional line of evidence for an early wet Mars.

#### 4.5. Influence of a Primordial Crust

[64] As discussed earlier, information derived from SNC meteorites suggests that a major differentiation of the mantle occurred very early in Mars' history [e.g., Harper *et al.*, 1995; Lee and Halliday, 1997], and this could have significant implications for the subsequent evolution of the planet. Hafnium-tungsten isotopic work [Lee and Halliday, 1997] suggests that the core differentiated rapidly (<45 Myr) and, because of the correlation between tungsten ( $^{182}\text{W}$ ) and neodymium ( $^{142}\text{Nd}$ ) [Harper *et al.*, 1995] anomalies, a primordial crust (of unknown thickness) formed coeval with this event. Such timing may be consistent with a crustal reservoir at the 4.5 Ga start time of our models. Blichert-Toft *et al.* [1999] have suggested that an early differentiation of the shergottite source region proceeded by extraction of small degree (fraction of a percent) partial melts in the presence of residual garnet. Small degree partial melting could lead to the pronounced enrichment of thorium relative to uranium (time-integrated) observed in Shergotty and Zagami compared to the other shergottites and potentially to their near-chondritic  $^{142}\text{Nd}$  and  $^{182}\text{W}$  anomalies, all of which could have been inherited during contamination of the primary magmas of these meteorites [Blichert-Toft *et al.*, 1999] by the products of this early melting. These arguments suggest an alternative, yet equally underconstrained, model of Mars' thermal and crustal evolution. This model includes the genesis of a primary/unrecycled crust that is enriched in heat-producing elements relative to the mantle and constitutes some unknown fraction of the present crustal volume. Norman [1999, 2002], on the basis of a Nd mass balance model, has suggested that this primary crust would most likely be  $\sim 20$ – $30$  km thick, but possibly  $10$ – $45$  km thick. Such a model, with a wet mantle and primary crustal enrichment up to 10 times the primitive Martian mantle, could satisfy a more strenuous application of the constraint that substantial crustal additions were completed by 4 Ga (Figure 12a–12c). Models with a dry mantle, however, tend to have any substantive secondary crustal additions initiate at  $\sim 3$  Ga, which is not consistent with the geologic record [e.g., Tanaka *et al.*, 1992] or the requirement that the preponderance of the crust was in place by  $\sim 4$  Ga [e.g., Phillips *et al.*, 2001b]. In addition, a dry mantle, with a crust that is 5–10 times more enriched than the primitive Martian mantle, may not lead to enough crustal additions to match the constraint of an average crustal thickness in the range of 50–100 km if the primary crust is <50 km thick. The large thermal lithospheric thicknesses during the early Noachian in these models may not be consistent with geophysical inferences of thin elastic lithospheres during that epoch either [e.g.,

Zuber *et al.*, 2000; P. J. McGovern *et al.*, Localized gravity/topography admittance and correlation spectra on Mars: Implications for regional and global evolution, submitted to *Journal of Geophysical Research*, 2002]. Models with an enriched primary crust are consistent with geochemical analyses of SNC meteorites, and they provide an additional mechanism by which the constraint that most major crustal additions were emplaced by 4 Ga can be satisfied.

### 5. Summary and Conclusions

[65] A simple, coupled thermal and magmatic model, where the energy involved in the thermodynamics of melting and differentiation of heat-producing isotopes is included, can match basic geophysical constraints on the history of Mars. Our nominal model generates a crust 62 km thick quite rapidly and has a core heat flux history that may be consistent with an early magnetic field that turned off early and is inactive today. A systematic investigation of multiple parameters also suggests (1) that the mantle is wet, (2) that the potassium content of the bulk silicate portion of the planet must be near chondritic, and (3) that an enriched primary crust provides a mechanism for strictly satisfying the constraint that most of the crust was in place by 4 Ga.

[66] Simple thermal evolution models for terrestrial planets typically involve solution of equations describing the conservation of energy with the help of a parameterization of the heat flux as a function of temperature via a Rayleigh number-Nusselt number relationship. Usually, these models strictly neglect the energetics of magma generation in their formulation [e.g., Phillips and Malin, 1983; Stevenson *et al.*, 1983; Schubert and Spohn, 1990]. While they may approximately include the effects of crustal differentiation and heat production [e.g., Phillips and Malin, 1983], most models neglect the latent energy needed to melt mantle materials and later released upon solidification. Though the energy related to the generation of crustal materials may represent only a few percent of the total energy budget, it plays a crucial role in controlling the volume of melt produced. Melting and convection processes cannot be energetically decoupled when investigating the internal thermal and magmatic evolution of moderately sized planetary bodies.

[67] As the rheology (and to a lesser degree, melting) of mantle materials is strongly governed by the abundance of water, so is the internal evolution of a planet. Thermomagmatic modeling of Mars' evolution indicates that a rheology sufficiently weakened by water is necessary to match constraints on crustal thickness and growth rates. Even modest estimates of mantle water content (e.g., 36 ppm) may provide a sufficiently weak upper mantle, though a greater abundance of water in the mantle may be more consistent with our models. Water delivery to the surface during early crustal genesis may provide an important source for driving early surface modification and climate on Mars.

[68] **Acknowledgments.** We would like to thank Andrew Dombard for a thorough review that greatly clarified an earlier version of this manuscript. Discussions with Sean Solomon and comments by Jeff Taylor and an anonymous reviewer were helpful in improving the paper. This research was supported by the NASA's Planetary Geology and Geophysics Program under grant NAG5-4448 to Washington University (PI: R.J.P.) and

final manuscript preparation by NAG5-4077 and NAG5-10165 to the Carnegie Institution of Washington (PI: S.C.S.).

## References

- Acuña, M. H., et al., Global distribution of crustal magnetization discovered by the Mars Global Surveyor MAG/ER experiment, *Science*, 284, 790–798, 1999.
- Albert, R. A., and R. J. Phillips, Paleoflexure, *Geophys. Res. Lett.*, 27, 2385–2388, 2000.
- Asimow, P. D., and E. M. Stolper, Steady-state mantle-melt interactions in one dimension, I, Equilibrium transport and melt focusing, *J. Petrol.*, 40, 475–494, 1999.
- Asimow, P. D., E. M. Stolper, and M. M. Hirschmann, An analysis of variations in isentropic melt productivity, *Philos. Trans. R. Soc. London, Ser. A*, 355, 255–281, 1995.
- Banerdt, W. B., and M. P. Golombek, Tectonics of the Tharsis region of Mars: Insights from MGS topography and gravity (abstract), *Lunar Planet. Sci.*, XXXI, 2038.pdf, 2000.
- Banin, A., B. C. Clark, and H. Wänke, Surface chemistry and mineralogy, in *Mars*, edited by H. H. Kieffer et al., pp. 594–625, Univ. of Ariz. Press, Tucson, 1992.
- Bertka, C. M., and Y. Fei, Mineralogy of the Martian interior up to core-mantle boundary pressures, *J. Geophys. Res.*, 102, 5251–5264, 1997.
- Bertka, C. M., and J. R. Holloway, Anhydrous partial melting of an iron-rich mantle, I, Subsolvus phase assemblages and partial melting phase relations at 10 to 30 kbar, *Contrib. Mineral. Petrol.*, 115, 313–322, 1994a.
- Bertka, C. M., and J. R. Holloway, Anhydrous partial melting of an iron-rich mantle, II, Primary melt compositions at 15 kbar, *Contrib. Mineral. Petrol.*, 115, 323–338, 1994b.
- Blichert-Toft, J., J. D. Gleason, P. Telouk, and F. Albarede, The Lu-Hf isotope geochemistry of shergottites and the evolution of the Martian mantle-crust system, *Earth Planet. Sci. Lett.*, 173, 25–39, 1999.
- Brownlow, A. H., *Geochemistry*, 580 pp., Prentice-Hall, Old Tappan, N. J., 1996.
- Carr, M. H., *Water on Mars*, 229 pp., Oxford Univ. Press, New York, 1996.
- Chen, J. H., and G. J. Wasserburg, Formation ages and evolution of Shergotty and its parent planet from U-Th-Pb systematics, *Geochim. Cosmochim. Acta*, 50, 955–968, 1986.
- Choblet, G., O. Grasset, E. M. Parmentier, and C. Sotin, Mars thermal evolution revisited, *Lunar Planet. Sci.*, XXXIX, 1556.pdf, 1999.
- Chopra, P. N., and M. S. Patterson, The role of water in the deformation of dunite, *J. Geophys. Res.*, 89, 7861–7876, 1984.
- Connerney, J. E. P., M. H. Acuña, P. J. Wasilewski, N. F. Ness, H. Rème, C. Mazelle, D. Vignes, R. P. Lin, D. L. Mitchell, and P. A. Cloutier, Magnetic lineations in the ancient crust of Mars, *Science*, 284, 794–798, 1999.
- Davaille, A., and C. Jaupart, Transient high Rayleigh number thermal convection with large viscosity variations, *J. Fluid Mech.*, 253, 141–166, 1993.
- DeSmet, J. H., A. P. van den Berg, and N. J. Vlaar, The evolution of continental roots in numerical thermo-chemical mantle convection models including differentiation by partial melting, *Lithos*, 48, 153–170, 1999.
- Dumoulin, C., M. P. Doin, and L. Fleitout, Heat transport in stagnant lid convection with temperature- and pressure-dependent Newtonian or non-Newtonian rheology, *J. Geophys. Res.*, 104, 16,293–16,302, 1999.
- Espósito, P. B., W. B. Banerdt, F. G. Lindal, W. L. Sjogren, M. A. Slade, B. G. Bills, D. E. Smith, and G. Balmino, Gravity and topography, in *Mars*, edited by H. H. Kieffer et al., pp. 209–248, Univ. of Ariz. Press, Tucson, 1992.
- Folkner, W. M., C. F. Yoder, D. N. Yuan, E. M. Standish, and R. A. Preston, Interior structure and seasonal mass redistribution of Mars from radio tracking of Mars Pathfinder, *Science*, 278, 1749–1751, 1997.
- Grasset, O., and E. M. Parmentier, Thermal convection in a volumetrically heated, infinite Prandtl number fluid with strongly temperature-dependent viscosity: Implications for planetary evolution, *J. Geophys. Res.*, 103, 18,171–18,181, 1998.
- Harper, C. L., Jr., L. E. Nyquist, B. Bansal, H. Weismann, and C.-Y. Shih, Rapid accretion and early differentiation of Mars indicated by  $^{142}\text{Nd}/^{144}\text{Nd}$  in SNC meteorites, *Science*, 267, 213–217, 1995.
- Hartmann, W. K., M. Malin, A. McEwen, M. Carr, L. Soderblom, P. Thomas, E. Danielson, P. James, and J. Veverka, Evidence for recent volcanism on Mars from crater counts, *Nature*, 397, 586–589, 1999.
- Hauck, S. A., II, and R. J. Phillips, Mars' dirty little secret (abstract), *Lunar Planet. Sci.*, XXXI, 1104.pdf, 2000.
- Hauck, S. A., II, R. J. Phillips, and A. M. Hofmeister, Variable conductivity: Effects on the thermal structure of subducting slabs, *Geophys. Res. Lett.*, 26, 3257–3260, 1999.
- Herzberg, C., P. Raterron, and J. Zhang, New experimental observations on the anhydrous solidus for peridotite KLB-1, *Geochem. Geophys. Geosyst.*, 1, Paper number 2000GC000089 [4498 words], 2000.
- Hirschmann, M. M., Mantle solidus: Experimental constraints and the effects of peridotite composition, *Geochem. Geophys. Geosyst.*, 1, Paper number 2000GC000070 [11,012 words], 2000.
- Hirschmann, M. M., P. D. Asimow, M. S. Ghiorso, and E. M. Stolper, Calculation of peridotite partial melting from thermodynamic models of minerals and melts, III, Controls on isobaric melt production and the effect of water on melt production, *J. Petrol.*, 40, 832–851, 1999.
- Hirth, G., and D. Kohlstedt, Water in the oceanic upper mantle: Implication for theology, melt extraction and the evolution of the lithosphere, *Earth Planet. Sci. Lett.*, 144, 93–108, 1996.
- Hofmeister, A. M., Mantle values of thermal conductivity and the geotherm from phonon lifetimes, *Science*, 283, 1699–1706, 1999.
- Hunten, D. M., Atmospheric evolution of the terrestrial planets, *Science*, 259, 915–920, 1993.
- Hynek, B. M., and R. J. Phillips, Evidence for extensive denudation of the Martian highlands, *Geology*, 29, 407–410, 2001.
- Johnson, M. C., M. J. Rutherford, and P. C. Hess, Chassigny petrogenesis: Melt compositions, intensive parameters, and water contents of Martian(?) magmas, *Geochim. Cosmochim. Acta*, 55, 349–366, 1991.
- Karato, S.-I., and P. Wu, Rheology of the upper mantle: A synthesis, *Science*, 260, 771–778, 1993.
- Karato, S.-I., M. S. Paterson, and J. D. Fitzgerald, Rheology of synthetic olivine aggregates—Influence of grain size and water, *J. Geophys. Res.*, 91, 8151–8176, 1986.
- Kavner, A., T. S. Duffy, and G. Shen, Phase stability and density of FeS at high pressures and temperatures: Implications for the interior structure of Mars, *Earth Planet. Sci. Lett.*, 185, 25–33, 2001.
- Kohlstedt, D. L., and M. E. Zimmerman, Rheology of partially molten mantle rocks, *Annu. Rev. Earth Planet. Sci.*, 24, 41–62, 1996.
- Kohlstedt, D. L., H. Keppler, and D. C. Rubie, Solubility of water in the  $\alpha$ ,  $\beta$ , and  $\gamma$  phases of  $(\text{Mg,Fe})_2\text{SiO}_2$ , *Contrib. Mineral. Petrol.*, 123, 345–357, 1996.
- Lee, D.-C., and A. N. Halliday, Core formation on Mars and differentiated asteroids, *Nature*, 388, 854–857, 1997.
- Lenardic, A., and L.-N. Moresi, Some thoughts on the stability of cratonic lithosphere: Effects of buoyancy and viscosity, *J. Geophys. Res.*, 104, 12,747–12,759, 1999.
- Leshin, L. A., Insights into Martian water reservoirs from analyses of Martian meteorite QUE94201, *Geophys. Res. Lett.*, 27, 2017–2020, 2000.
- Lodders, K., and B. Fegley, An oxygen isotope model for the composition of Mars, *Icarus*, 126, 373–394, 1997.
- Lodders, K., and B. Fegley, *The Planetary Scientist's Companion*, 371 pp., Oxford Univ. Press, New York, 1998.
- Mackwell, S. J., High-temperature rheology of enstatite: Implications for creep in the mantle, *Geophys. Res. Lett.*, 18, 2027–2030, 1991.
- Mackwell, S. J., D. L. Kohlstedt, and M. S. Paterson, The role of water in the deformation of olivine single crystals, *J. Geophys. Res.*, 90, 11,319–11,333, 1985.
- Mackwell, S. J., M. E. Zimmerman, and D. L. Kohlstedt, High-temperature deformation of dry diabase with application to tectonics on Venus, *J. Geophys. Res.*, 103, 975–984, 1998.
- McDonough, W. F., and S.-S. Sun, The composition of the Earth, *Chem. Geol.*, 120, 223–253, 1995.
- McKenzie, D. P., The generation and compaction of partial melts, *J. Petrol.*, 25, 713–765, 1984.
- McKenzie, D. P., and M. J. Bickle, The volume and composition of melt generated by extension of the lithosphere, *J. Petrol.*, 29, 625–679, 1988.
- McLennan, S., Crustal heat production and the thermal evolution of Mars, *Geophys. Res. Lett.*, 28, 4019–4022, 2001.
- McNutt, M. K., Lithospheric flexure and thermal anomalies, *J. Geophys. Res.*, 89, 11,180–11,194, 1984.
- McSween, H. Y., What have we learned about Mars from SNC meteorites?, *Meteoritics*, 29, 757–779, 1994.
- McSween, H. Y., T. L. Grove, R. C. F. Lentz, J. C. Dann, A. H. Holzheid, L. R. Riciputi, and J. G. Ryan, Geochemical evidence for magmatic water within Mars from pyroxenes in the Shergotty meteorite, *Nature*, 409, 487–490, 2001.
- Mei, S., and D. L. Kohlstedt, Influence of water on plastic deformation of olivine aggregates, 1, Diffusion creep regime, *J. Geophys. Res.*, 105, 21,457–21,470, 2000a.
- Mei, S., and D. L. Kohlstedt, Influence of water on plastic deformation of olivine aggregates, 2, Dislocation creep regime, *J. Geophys. Res.*, 105, 21,471–21,482, 2000b.
- Moresi, L.-N., and V. S. Solmatov, Mantle convection with a brittle lithosphere: Thoughts on the global tectonic styles of Earth and Venus, *Geophys. J. Int.*, 133, 669–682, 1998.

- Mysen, B. O., D. Virgo, R. K. Popp, and C. M. Bertka, The role of H<sub>2</sub>O in Martian magmatic systems, *Am. Mineral.*, *83*, 942–946, 1998.
- Nimmo, F., and D. J. Stevenson, Influence of early plate tectonics on the thermal evolution and magnetic field of Mars, *J. Geophys. Res.*, *105*, 11,969–11,980, 2000.
- Norman, M., The composition and thickness of the crust of Mars estimated from rare earth elements and neodymium-isotopic compositions of Martian meteorites, *Meteorit. Planet. Sci.*, *34*, 439–449, 1999.
- Norman, M., The composition and thickness of the Martian crust revisited: Implications of an ultradepleted mantle with a Nd isotopic composition like that of QUE94201 (abstract), *Lunar Planet. Sci.*, XXXIII, 1175.pdf, 2002.
- Ogawa, M., A numerical model of the coupled magmatism-mantle convection system in Venus and the Earth's mantle beneath Archean continental crusts, *Icarus*, *102*, 40–61, 1993.
- Phillips, R. J., and V. L. Hansen, Geological evolution of Venus: Rises, plains, plumes, and plateaus, *Science*, *279*, 1492–1497, 1998.
- Phillips, R. J., and M. C. Malin, The interior of Venus and tectonic implications, in *Venus*, edited by D. M. Hunten et al., pp. 159–214, Univ. of Ariz. Press, Tucson, 1983.
- Phillips, R. J., M. A. Bullock, and S. A. Hauck II, Coupled climate and interior evolution of Venus, *Geophys. Res. Lett.*, *28*, 1779–1782, 2001a.
- Phillips, R. J., M. T. Zuber, S. C. Solomon, M. P. Golombek, B. M. Jakosky, W. B. Banerdt, R. M. Williams, B. Hynke, O. Aharonson, and S. A. Hauck II, Ancient geodynamics and global-scale hydrology on Mars, *Science*, *291*, 2587–2591, 2001b.
- Ranalli, G., *Rheology of the Earth*, 413 pp., Chapman and Hall, New York, 1995.
- Reddy, J. N., and D. K. Gartling, *The Finite Element Method in Heat Transfer and Fluid Dynamics*, 390 pp., CRC Press, Boca Raton, Fla., 1994.
- Reese, C. C., V. S. Solomatov, and L.-N. Moresi, Heat transport efficiency for stagnant lid convection with dislocation viscosity: Application to Venus and Mars, *J. Geophys. Res.*, *103*, 13,643–13,658, 1998.
- Reese, C. C., V. S. Solomatov, and L.-N. Moresi, Non-Newtonian stagnant lid convection and magmatic resurfacing on Venus, *Icarus*, *139*, 67–80, 1999.
- Ruzicka, A., G. A. Snyder, and L. A. Taylor, Comparative geochemistry of basalts from the Moon, Earth, HED asteroid, and Mars: Implications for the origin of the Moon, *Geochim. Cosmochim. Acta*, *65*, 979–997, 2001.
- Sanloup, C., A. Jambon, and P. Gillet, A simple chondritic model of Mars, *Phys. Earth Planet. Int.*, *112*, 43–54, 1999.
- Schatz, J. F., and G. Simmons, Thermal conductivity of earth materials at high temperatures, *J. Geophys. Res.*, *77*, 6966–6983, 1972.
- Schmerr, N. C., Y. Fei, and C. M. Bertka, Extending the solidus for a model iron-rich Martian mantle composition to 25 GPa (abstract), *Lunar Planet. Sci.*, XXXII, 1157.pdf, 2001.
- Schubert, G., and T. Spohn, Thermal history of Mars and the sulfur content of its core, *J. Geophys. Res.*, *95*, 14,095–14,104, 1990.
- Schubert, G., S. C. Solomon, D. L. Turcotte, M. J. Drake, and N. H. Sleep, Origin and thermal evolution of Mars, in *Mars*, edited by H. H. Kieffer et al., pp. 147–183, Univ. of Ariz. Press, Tucson, 1992.
- Schubert, G., V. S. Solomatov, P. J. Tackley, and D. L. Turcotte, Mantle convection and the thermal evolution of Venus, in *Venus II-Geology, Geophysics, Atmosphere, and Solar Wind Environment*, edited by S. W. Bougher, D. M. Hunten, and R. J. Phillips, pp. 1245–1287, Univ. of Ariz. Press, Tucson, 1997.
- Sleep, N., Martian plate tectonics, *J. Geophys. Res.*, *99*, 5639–5656, 1994.
- Sleep, N., Evolution of the mode of convection within terrestrial planets, *J. Geophys. Res.*, *105*, 17,563–17,578, 2000.
- Smith, D. E., et al., The global topography of Mars and implications for surface evolution, *Science*, *284*, 1495–1503, 1999.
- Sohl, F., and T. Spohn, The interior structure of Mars: Implications from SNC meteorites, *J. Geophys. Res.*, *102*, 1613–1635, 1997.
- Solomatov, V. S., Scaling of temperature- and pressure-dependent viscosity convection, *Phys. Fluids*, *7*, 266–274, 1995.
- Solomatov, V. S., and L.-N. Moresi, Stagnant lid convection on Venus, *J. Geophys. Res.*, *101*, 4737–4753, 1996.
- Solomatov, V. S., and L.-N. Moresi, Scaling of time-dependent stagnant lid convection: Application to small-scale convection on Earth and other terrestrial planets, *J. Geophys. Res.*, *105*, 21,795–21,817, 2000.
- Solomon, S. C., Formation, history and energetics of cores in the terrestrial planets, *Phys. Earth Planet. Int.*, *19*, 168–192, 1979.
- Solomon, S. C., and J. W. Head, Heterogeneities in the thickness of the elastic lithosphere of Mars-Constraints on heat flow and internal dynamics, *J. Geophys. Res.*, *95*, 11073–11083, 1990.
- Stevenson, D. J., T. Spohn, and G. Schubert, Magnetism and thermal evolution of the terrestrial planets, *Icarus*, *54*, 466–489, 1983.
- Tanaka, K. L., D. H. Scott, and R. Greeley, Global stratigraphy, in *Mars*, edited by H. H. Kieffer et al., pp. 345–382, Univ. of Ariz. Press, Tucson, 1992.
- Turcotte, D. L., and G. Schubert, *Geodynamics*, 450 pp., John Wiley, New York, 1982.
- van den Berg, A. P., D. A. Yuen, and V. Steinbach, The effects of variable thermal conductivity on mantle heat-transfer, *Geophys. Res. Lett.*, *28*, 875–878, 2001.
- Wänke, H., and G. Dreibus, Chemistry and accretion of Mars, *Philos. Trans. R. Soc. London, Ser. A*, *349*, 2134–2137, 1994.
- Weizman, A., D. J. Stevenson, D. Prialnik, and M. Podolak, Modeling the volcanism on Mars, *Icarus*, *150*, 195–205, 2001.
- Zhang, J., and C. Herzberg, Melting experiments on anhydrous peridotite KLB-1 from 5.0 to 22.5 GPa, *J. Geophys. Res.*, *99*, 17,729–17,742, 1994.
- Zhong, S., and M. T. Zuber, Long-wavelength topographic relaxation for self-gravitating planets and implications for the time-dependent compensation of surface topography, *J. Geophys. Res.*, *105*, 4153–4164, 2000.
- Zhong, S., and M. T. Zuber, Degree-1 mantle convection and the crustal dichotomy on Mars, *Earth Planet. Sci. Lett.*, *189*, 75–84, 2001.
- Zuber, M. T., et al., Internal and early thermal evolution of Mars from Mars Global Surveyor topography and gravity, *Science*, *287*, 1788–1793, 2000.

S. A. Hauck II, Department of Terrestrial Magnetism, Carnegie Institution of Washington, 5241 Broad Branch Road NW, Washington, DC 20015. (hauck@dtm.ciw.edu)

R. J. Phillips, McDonnell Center for the Space Sciences, Department of Earth and Planetary Sciences, Washington University, One Brookings Drive, Campus Box 1169, St. Louis, MO 63130. (phillips@wustite.wustl.edu)